

Environmental design solutions for existing concrete flat roofs in low-cost housing to improve passive cooling in western Mexico

GARCÍA-SOLÓRZANO, Luis A, ESPARZA-LOPEZ, Carlos J and AL-OBAIDI, Karam <<http://orcid.org/0000-0002-4379-6964>>

Available from Sheffield Hallam University Research Archive (SHURA) at:

<https://shura.shu.ac.uk/27116/>

This document is the Accepted Version [AM]

Citation:

GARCÍA-SOLÓRZANO, Luis A, ESPARZA-LOPEZ, Carlos J and AL-OBAIDI, Karam (2020). Environmental design solutions for existing concrete flat roofs in low-cost housing to improve passive cooling in western Mexico. Journal of Cleaner Production. [Article]

Copyright and re-use policy

See <http://shura.shu.ac.uk/information.html>

Environmental design solutions for existing concrete flat roofs in low-cost housing to improve passive cooling in western Mexico

Luis A. García-Solórzano ^a, Carlos J. Esparza-Lopez ^a, Karam M. Al-Obaidi ^{b,*}

^a Faculty of Architecture and Design, University of Colima, Mexico

^{b*} Department of the Natural and Built Environment, College of Social Sciences and Arts, Sheffield Hallam University, Sheffield, UK

Abstract

The development of real estate in Mexico has largely ruled out the comfort of users that focused on economic matters and made it difficult to make substantial progress in adopting measures to improve indoor environmental quality. Current research projects in Mexico found that roof construction in low-cost housing struggles to meet the requirements of the indoor climate. Passive cooling strategies are techniques to control heat gain and heat dissipation in buildings to maximise the comfort and health of building users while minimising energy use. Passive cooling systems recognize climate conditions and utilise renewable sources of energy such as the sun and wind to provide cooling and ventilation. Therefore, this study aims to develop a green and sustainable solution for existing concrete flat roofs with no major interventions and investments to save energy. The design of a passive device was tested to assess its effectiveness to protect flat roofs from shortwave radiation and to allow for heat dissipation in Mexican buildings. The study used a quantitative approach based on experiments and simulation tests to evaluate design efficiency. The results showed that a perforated device with an opening percentage of 88% and a cavity of 0.05m between the roof and the device provided effective protection. Also, the device with blinds of 45° showed lower operative temperatures within a range of mean values between 0.8°C and 0.9°C compared to a roof with a full shade cover in the hot and humid season. However, the perforated device with blinds of 90° in black colour delivered the best performance compared to other models and recorded a mean value of 1.13°C in the hot sub-humid season. The results revealed the efficiency of the proposed device that can be observed within different geometric configurations, surface properties as well as the use of the nocturnal radiative cooling potential in blocking solar radiation in Mexican buildings.

Keywords: radiative cooling; flat roof; passive cooling; solar shading; hot and humid climate; Mexico

1. Introduction

Energy consumption in cities significantly increases due to rapidly expand in urbanization and grow in population activities that contribute to accelerating gas emissions, increasing air temperatures and intensifying urban heat island (UHI) effect (Frayssinet et al., 2018). The case of Mexico is no exception, as it is made up of a society that has a significant population explosion with about 120 million inhabitants in 2015 (National Institute of Geography and Informatics Statistics, 2015). World Energy Statistics showed that a significant percentage of energy consumption is directly related to

the operation of the buildings, these demands vary depending on the weather and the minimum considerations that are taken for the appropriate design (Li and Wang, 2020). In Mexico, McNeil et al. (2018) stated that electricity use jumps by 30% each summer as Mexican homes and businesses turn on their air conditioners. The report indicated nearly half of cooling electricity is used in homes and it costs Mexican consumers about 31 billion pesos annually and incurs another 46 billion pesos in government subsidies in the residential sector. Also, the report revealed that in the warmest regions, cooling energy in hot months responsible for over half of peak electricity demand. The report also stated that GHG emissions from cooling are expected to double up and expected to reach 20 million tons by 2030. By 2050, peak-load from cooling is expected to grow by 26 GW. Although Mexico could depend on solar electricity, it has been found that much of the cooling peak occurs late at night when solar is unavailable and wind output is lower.

In spite of the fact that real estate development in Mexico focused on economic matters, this development has made it difficult to make substantial progress in adopting measures to support energy demand without affecting the local environment (INECC, 2015). Housing institutes in Mexico, such as Institute of the National Housing Fund for Workers (INFONAVIT) and Housing Fund of the Institute for Social Security and Services of State Workers (FOVISSSTE) have incorporated programs and strategies that encourage environmental respect and the use of ecotechnologies in housing products that are offered under its guidelines. However, these programs have provided basic considerations of human comfort through design, as most strategies rely on the use of efficient HVAC systems, solar water heaters, or water savings faucets instead of considering bioclimatic design strategies to improve indoor thermal environments (Martinez-Torres, 2017; Acosta, 2018; González-Yñigo, 2018). On the other hand, the National Housing Commission (CONAVI, 2015) indicated that 153411 houses in Colima were built of concrete roofs and with no strategies of proper insulation and protection from outdoor environments. In fact, there are numerous housing projects built with minimal strategies of passive design that failed to provide protection from the impact of the local climate (Esparza, 2015; Feng et al., 2019).

In the report of the characteristics of the inhabited private dwellings in the western part of Mexico, the National Housing Commission (CONAVI, 2015) showed that the dominant roofing types in dwellings are concrete slabs and metal sheets with 75.07% and 12.77%, respectively. This trend has been maintained in recent years, making concrete surfaces the most dominant type of construction in western Mexico. In addition, the urban configuration that prevails in the locality causes most of low-cost housing projects to be formed in groups that shaped as continuous sets of flat roofs. This construction has triggered negative consequences on the inhabitants of these houses that even correlated with domestic violence (Gómez et al., 2005).

Many studies indicated that the roof considers as a significant building element where most heat gain occurs particularly in low rise buildings (Al-Obaidi et al. 2014b; Yang et al., 2018; Esparza et al., 2018; Zhang et al., 2019), especially the external surfaces that consider crucial in roofing design (Pisello et al., 2015; Schabbach et al., 2018; Shariati et al., 2019c). This study reviewed different environmental roofing systems based on various methods via mathematical models followed by studies with empirical tests then mixed methods between mathematical and experimental models (Table 1).

Table 1: Previous studies conducted on mathematical models, experimental methods and experimental with mathematical methods on developing environmental roofing systems.

No.	Authors	Country	Climate	Type	Methodology
1	Harold and Yellott (1969)	USA	Arid	Skytherm	Experimental Methods
2	Givoni (1977)	Israel	Arid	Radiation Trap	Experimental Methods
3	Kimball (1985)	USA	Arid	Flat Radiator	Experimental and Mathematical Methods
4	González (1997)	Venezuela	Hot and Humid	ESUCE-AC Skytherm	Experimental Methods
5	Mihalakakou et al. (1998)	Italy	Temperate oceanic	Metal Radiator	Experimental and Mathematical Methods
6	Erell and Etzion (2000)	Israel	Arid	Flat Radiator	Mathematical Models
7	González (2002)	Venezuela	Hot and Humid	Radiative Cooling	Experimental Methods
8	Nahar et al. (2003)	India	Hot and Dry	White paint Vermiculite Isolation Night cooling Air insulation Pond roof White glazed tile	Experimental Methods
9	Frigerio (2004)	Argentina	Temperate oceanic	Metal Radiator	Experimental and Mathematical Methods
10	Parker (2005)	U.S.A.	Various	Metal Radiator	Mathematical Models
11	Dimoudia and Androutopoulos (2006)	Greece	Temperate and Mediterranean	Rooftop Radiator with Water	Experimental Methods
12	Bagiorgas and Mihalakakou (2007)	Greece	Temperate and Mediterranean	Metal Radiator	Experimental and Mathematical Methods
13	Herrera (2009)	México	Hot and Dry	Evaporation Cooling	Experimental Methods
14	Heidarinejad et al. (2010)	Iran	Hot and Dry	Flat Radiator	Mathematical Models
15	Zhang and Niu (2012)	China	Various	Radiator MPCHM	Experimental and Mathematical Methods
16	Hollick (2012)	Canada	Humid continental	Metal Radiator	Experimental Methods
17	González and González (2013)	Venezuela	Humid	Pond Roof	Experimental Methods
18	Al-Obaidi et al. (2014b)	Malaysia	Hot and Humid	Ventilated attic, radiative and reflective roof	Experimental Methods
19	Al-Obaidi et al. (2014c)	Malaysia	Hot and Humid	Radiative and Reflective Roofs	Experimental and Mathematical Methods
20	Hanif et al. (2014)	Malaysia	Hot and Humid	Flat Radiator	Mathematical Models
21	Sabzi et al. (2015)	Iran	Arid	Pond Roof, Water Bags and Radiation Shield	Experimental and Mathematical Methods

22	Tevar et al. (2015)	Spain	Hot semi-arid	Emissivity	Experimental and Mathematical Methods
23	Man et al. (2015)	China	Humid sub-tropical	Metal radiator	Experimental and Mathematical Methods
24	Al-Obaidi et al. (2016)	Malaysia	Hot and Humid	Ventilation and thermal	Experimental Methods
25	Yew et al. (2018)	Malaysia	Hot and Humid	Cavity ventilation and thermal reflective coating	Experimental Methods
26	Esparza et al. (2018)	Mexico	Hot sub-humid	Roof pond, floating fibre (gunny bags) and wet fibre	Experimental and Mathematical Methods
27	Almodovar and La Roche (2019)	Spain	Hot semi-arid	Roof ponds combined with a water-to-air heat exchanger	Experimental and Mathematical Methods

In 1959, Head proposed for the first time the use of selective infrared emitters during the night to improve the effect of radiative cooling, since then researchers have made proposals to use it with different applications (Zehighami et al., 2018). In the 60's and 70's, Hay and Yellott (1969) used the Skytherm system (Figure 1) with six ways to model the environmental conditions via solar heating, thermal capacity, night radiation, water evaporation, radiation, evaporation and fan-coil system. The results achieved average indoor temperatures between 21°C and 26.6°C for an entire year without the need for additional heating or cooling loads, while outside temperatures were between the freezing point and 46°C, the system managed to demonstrate high efficiency, however, the involvement of mechanical and electrical devices to operate the openings and closures of the cover made it more expensive. Givoni (1977) proposed a system called it a Roof Radiation Trap, which uses solar energy for heating buildings in the winter and night radiation for cooling in summer. In later years, several authors continued to explore the phenomenon of radiative cooling as a passive strategy, mainly in dry climates where the potential is greater.

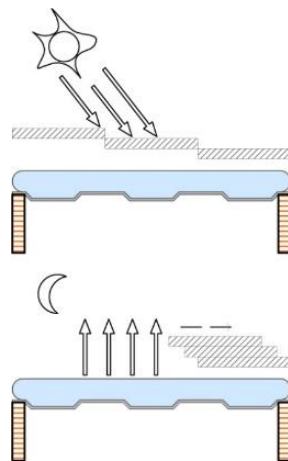


Figure 1: Illustrations of Skytherm system (Hay and Yellott, 1969)

Studies with mathematical models such as Erell and Etzion (2000) tested solar collectors as night radiators to cool fluids that investigated the influence of the exposed area of the radiator with convection exchange. Parker (2005) reported that the variables with the greatest influence on cooling performance were: outdoor air temperature, dew point temperature, cloudiness and wind speed (Figure 2). Heidarinejad et al. (2010) presented the importance of night radiative cooling as a

factor that increases the effectiveness of a hybrid system by up to more than 100% in a dry climate (Figure 3). In the hot humid climate, Hanif et al. (2014) achieved 25% energy saving for cooling purposes and mentioned the opportunity of night radiative cooling.

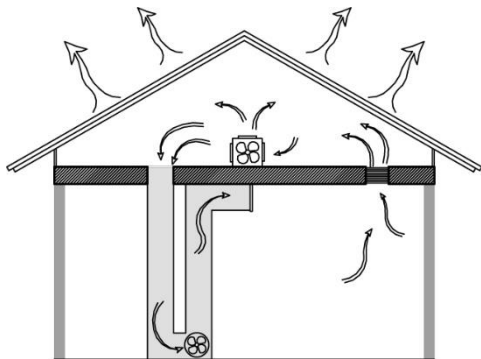


Figure 2: Night cooling scheme (Parker, 2005)

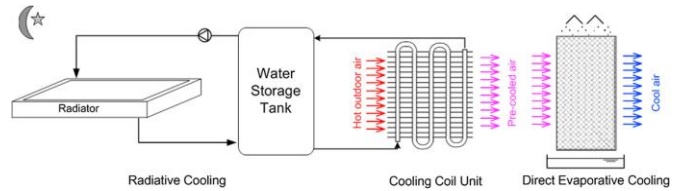


Figure 3: Schematic diagram of hybrid radiative cooling system (Heidarinejad et al., 2010).

Studies with experimental methods such as González (1997) who used a pond and dry surfaces with controlled insulation in a Skytherm system with some operational differences in humid weather. Subsequently, at the same location, González (2002) applied a system consists of sheets that function as night radiators whereas its operation achieved comparable temperatures to the average daily air temperature of the surroundings (Figure 4). Nahar et al. (2003) tested several systems to achieve night cooling in experimental models in summer, a significant difference was recorded with the use of evaporative cooling, followed by using white tiles. However, when considering the operation and water requirements, it was found that tiles were preferred to be applied over roofs in dry weather (Figure 5). Dimoudia and Androutsopoulos (2006) evaluated a night-time radiator that uses water as an exchange fluid and observed material properties to achieve greater efficiency in night cooling (Figure 6).

Herrera (2009) observed the importance of sun protection in cooling strategies, as a result, Hollick (2012) found that using a metal radiator in a clear night helped to provide cooling effect where the surface temperature was 10°C below room temperature and the indoor air temperature was lower 4.7°C compared to the conventional room in a humid-continental climate (Figure 7). González and González (2013) studied a system that combined cooling systems with thermal mass in the humid climate and they found that radiative cooling strategy helped the system to increase its efficiency, but as also increases the complexity of its operation (Figure 8). Al-Obaidi et al. (2014b) developed a ventilated attic system with a reflective and radiative roof that included skylight to reduce the heat impact from solar light in low rise buildings in a hot and humid climate (Figure 9). By combining reflective, radiative and ventilation strategies, they managed to lower indoor air by up to 2.01°C during the day compared to a traditional attic.

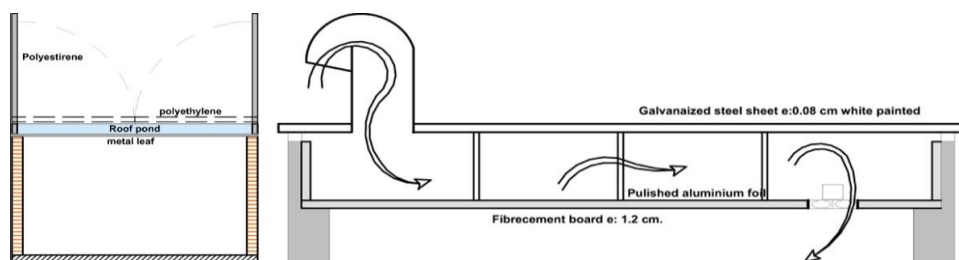


Figure 4: Dry surface and pond with controlled insulation and convective and radiant cooling systems system (González, 2002)

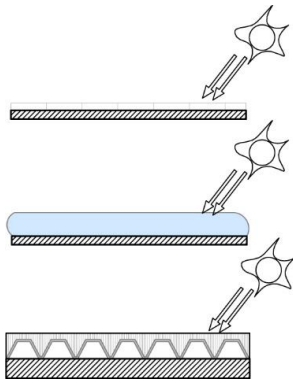


Figure 5: Roof cooling systems (Nahar et al., 2003)

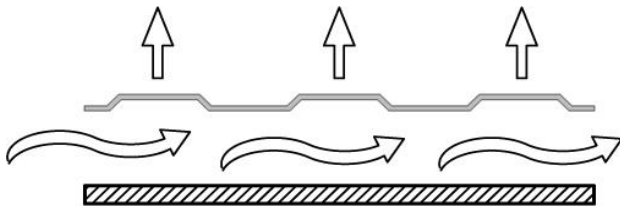


Figure 7: Metal radiator (Hollick, 2012)

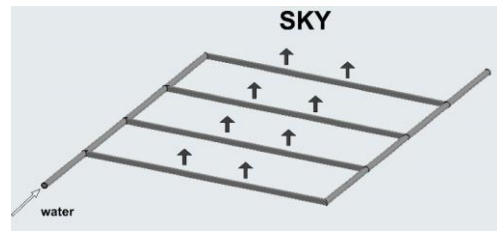


Figure 6: Water radiator (Dimoudia & Androutsopoulos, 2006)

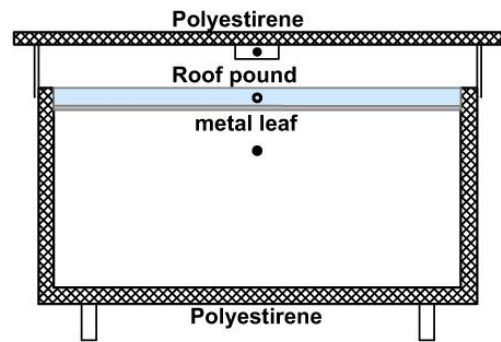


Figure 8: Pond roof (González & González, 2013)

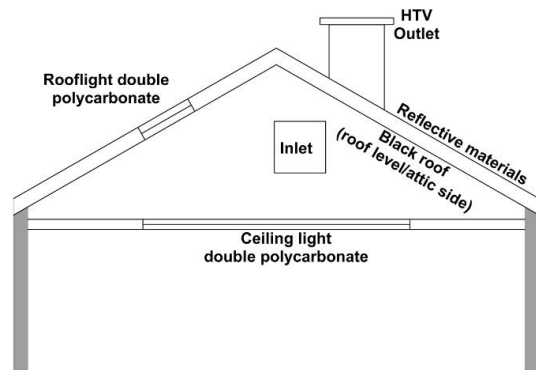


Figure 9: Innovative roofing system (Al-Obaidi et al., 2014b)

Experimental and mathematical methods have been developed and demonstrated by previous studies such as Kimbal (1985) who monitored aluminium radiators of applied white TiO₂ paint, normal black paint, and black paint with polyethylene layer. Higher energy losses were observed in the black paint that had no convective protection also it was observed that moisture and cloudiness were recognized as factors that reduces the efficiency of a radiator. Frigerio (2004) conducted measurements in a temperate climate to estimate the emissivity of the sky and its cooling potential. Duarte et al. (2006) performed an analysis between measurements and equations by statistical methods (BIAS, RMSE, MAE, PMRE) to determine the best equation for clear skies and cloudy skies in a tropical region of Brazil. Bagiorgas and Mihalakakou (2008) made a comparison between radiators with an emissivity of 0.71 and 0.93, experimentally and theoretically (Figure 10), correlations were also made between the experimental and theoretical models, it was found that there is a high agreement also between the theoretical and experimental temperatures of the radiator that have high emissivity. Zhang and Niu (2012) combined the use of a microencapsulated phase change material with a night cooling system, the results indicated that this system has little effect in a hot and humid climate (Figure 11). Sabzi et al, (2015) compared three passive cooling systems: rooftop

water tank, rooftop water bag and radiation shield. The results indicated that the best performance was of the rooftop water tank, followed by the radiation shield that implies less complexity in its adoption (Figure 12). Tevar et al. (2015) compared the cooling potential of convective radio panels with emittance values of 0.02, 0.5 and 0.9, the results were consistent with what was expected as an increase in an emittance value better performance can be achieved. Man et al, (2015) used a metallic night radiator on the roof that was evaluated as a complement to the active system in the hot and humid climate. The experiment was verified by simulation and with a radiator model built with double glazed carbonate sheets (Figure 13).

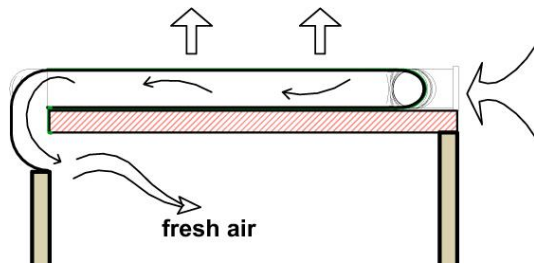


Figure 10: Radiator model (Bagiorgas and Mihalakou, 2008)

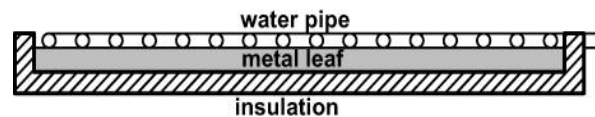


Figure 11: Cooling system with phase change material (Zhang and Niu, 2012)

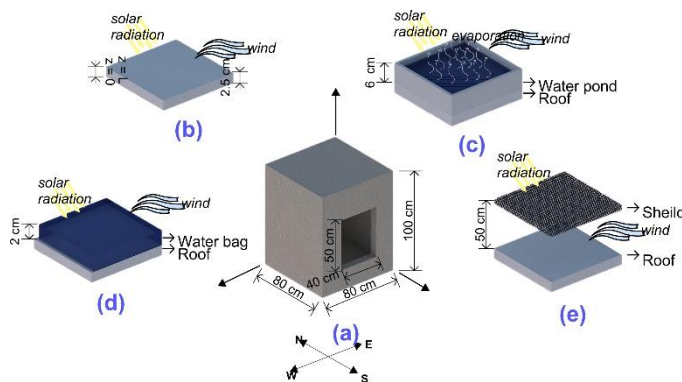


Figure 12: Roof cooling systems (Sabzi et al., 2015)

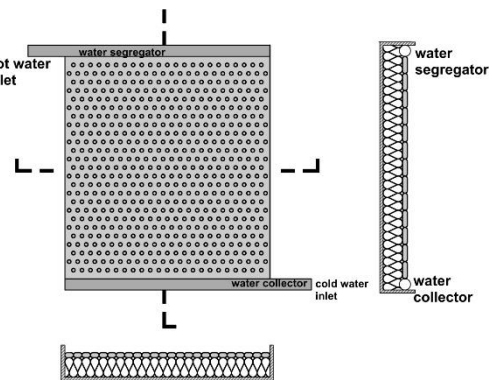


Figure 13: Ceiling night radiator (Man et al., 2015)

Background of investigations carried out on surface properties showed various techniques implemented to use the surfaces properties with the purpose of increasing the performance and durability of building envelopes (Imran et al., 2018; Shariati et al., 2019b). Orel B. et al. (1993) monitored radiative surfaces in test cells by using paints on an aluminium substrate, found improvements in cooling with the application of Barium sulfate $BaSO_4$, at $3.2^\circ C$. Syneffa et al. (2006) found that the spectral reflectance during the day and the infrared emittance at the night are the factors that influence a better thermal performance of the selected surfaces. On the other hand, Raman et al. (2014) presented an innovative device that works as a solar reflector and thermal emitter, which consists of a film composed of nanometric layers of Hafnium Dioxide HfO_2 and Silicon Dioxide SiO_2 that reflects 97% of the solar light and that in full sunbeam can cool down to $4.9^\circ C$ below room temperature. In a review of roofing techniques in tropical houses in Southeast Asia, Al-Obaidi et al. (2014a and 2014c) considered the radiative and reflective techniques as methods to reduce heat gains from the roof. In the application of convection covers of surfaces exposed to heat exchange, Bosi et al (2014) developed a proposal for a zinc sulphide film that replaces polyethylene. In a review of night cooling systems, Nwaigwe et al (2010) grouped water cooling systems and air-

cooling systems, as well as studies to determine the net radiation of the sky in different places. It presented experiences of field tests and the difficulties to popularize these systems.

With climatic conditions as in Colima, Guarneros et al. (2012) stated that the components for the operation of a cooling system should cover a space for cooling, a heat dissipator and a heat sink. However, the difficulty involved in the use of passive radiative cooling systems due to thermal gradient, cloud cover and moisture content that control the passage of long-wave radiation towards the sky. These problems are exacerbated in the summer with longer daylight periods and heavy rain, however, in the winter with longer nights and less rainfall, it is conducive to increase cooling. The relevance of the subject is reinforced by the constant expression of user discomfort in this type of housing (Esparza, 2015).

It is important to develop a proposal that does not require many interventions and large investments. As a result, this development demands a solution of low impact technology (González, 2011; Shao et al., 2018) that needs to be developed initially through empirical processes then it gradually adapts with the new uses. Consequently, the construction advancements could convert it into technical applications that could be replicated as part of a building. Therefore, this work proposes to implement and evaluate a passive system that works as a device that protects from direct solar radiation and to allow heat loss by night cooling. A passive device is proposed as a roof cover that meets the design features of low-cost housing developments in Mexico. The development of this research would help to set strategies for the improvement of low-cost housing in terms of energy savings and the reduction of carbon footprint.

2. Methodology

Based on the previous studies as mentioned in the introduction, the climatic and geographic conditions of the hot and humid climate show that there are difficulties in the implementation of nocturnal radiative cooling as a passive mean. Taking this issue, this research was conducted with an aim to evaluate the potential of a system that combines the blockade of short-wave radiation to avoid gains of heat during the day and allow heat loss by longwave radiation at the night. The study used a technique that combines high solar reflectance and high thermal emittance. The use of an appropriate reflective covering can significantly reduce the temperature of a surface, however, it is necessary to consider that not only colour but also the spectral reflectance (Synnefa et al., 2006) that affects its performance in the day and its emissivity that becomes important at the night. On the other hand, beyond the surface properties of the roof, solar protection would help to minimize the heat flux into space. Several studies mentioned the importance of solar blocking and the reduction of heat flux (D’Orazio et al. 2010; Almodovar and La Roche, 2019). Therefore, this study aims to analyse a passive cooling system that works through a device that protects from short wave radiation and allows the loss of heat by night cooling.

Therefore, this research applied a quantitative approach which was conducted in two stages, the first phase started with the implementation of a pre-experiment. The second phase was carried out through simulations where the independent variables were manipulated in a controlled environment that was monitored and analysed. A methodological scheme was developed and divided into two levels. The first level consists of the design and characterization of the shading device with the elaboration of a virtual cell. The second level is the simulations of the application with a device over the experimental cell.

2.1 Study Area

The study area is located in the western region of Mexico in the state of Colima. The predominant climate in the state is warm sub-humid and hot and humid with rains in summer, (winter rain less than 5%). The specific area is the municipality of Coquimatlán, which is located in the centre of the state of Colima, between 19°11'52" north latitude and 103°48'41" west longitude (Figure 14). The weather conditions of the study area do not experience extreme oscillations throughout the year. In the study area, the following annual temperatures are frequent with a maximum temperature of 34.6°C, an average of 26.6°C and a minimum of 18.7°C.

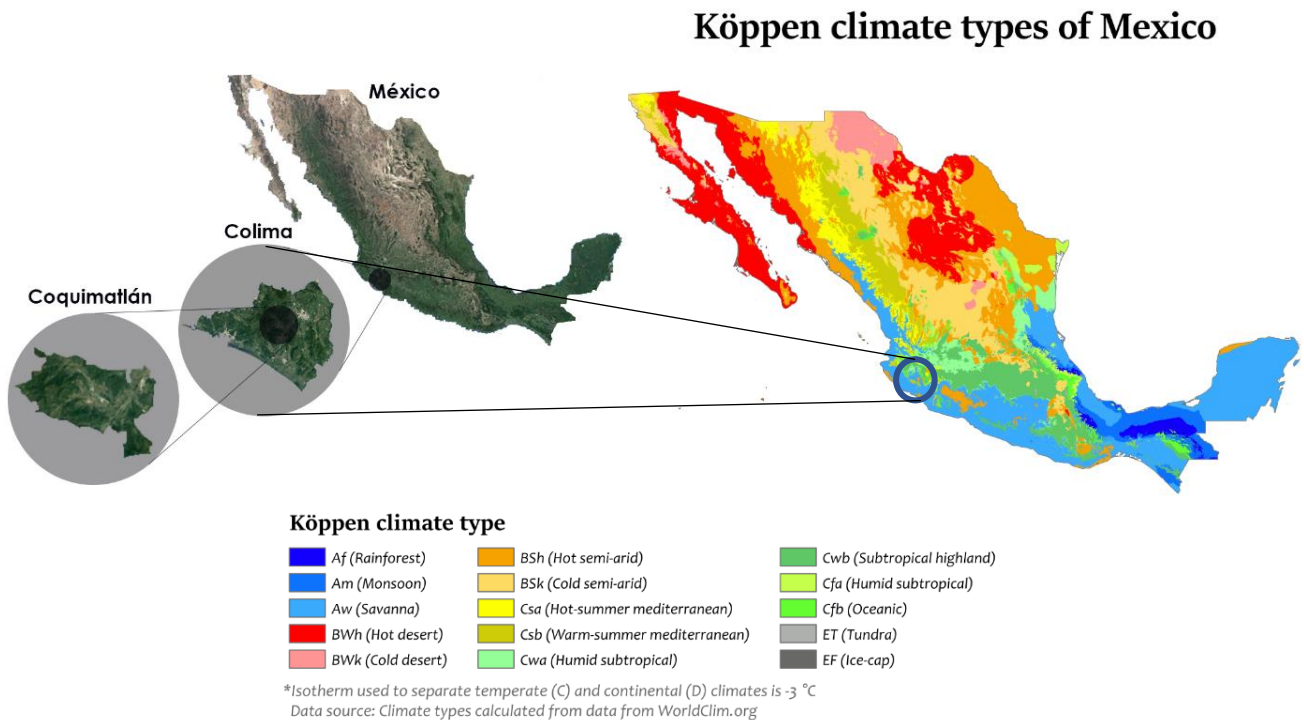


Figure 14: Maps of climates in the Mexican republic and location of the reference area.

Figure 15 shows readings of dry bulb temperatures (°C) and relative humidity (RH%) for a year in three climatic seasons that are defined and presented in three different colours. The orange zone is for the warm sub-humid season from January to April with an average temperature of 26.5°C and an average RH of 43%. The red zone is for the hot sub-humid season in May, June and December with an average temperature of 27.8°C and an average RH of 46.5%. Finally, the green zone is the hot humid season with an average temperature of 29.5 °C and an average RH of 55%.

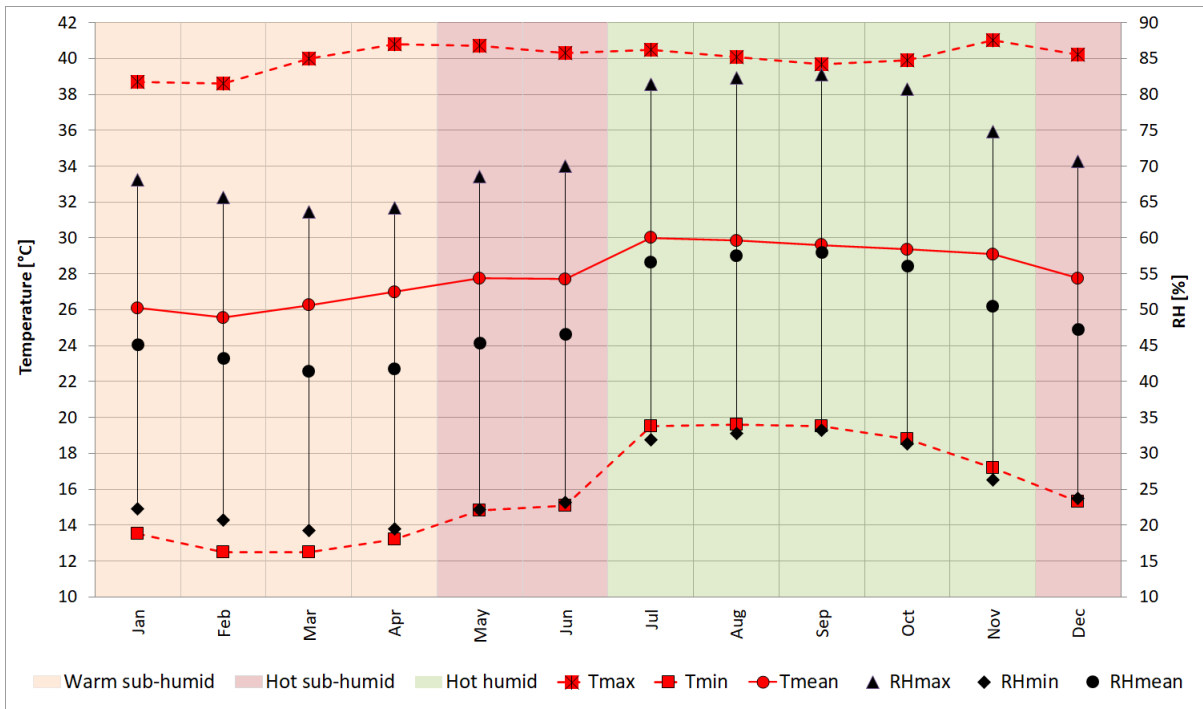


Figure 15: Dry bulb temperature and external relative humidity of the study area.

2.2 Experimental models

The experimental models were built at the Faculty of Architecture and Design of the University of Colima which located north of the Coquimatlán Delegation No. 4 campus with an arrangement consists of 12 blocks oriented 36° NE, with similar characteristics and aligned in two symmetrical axes with a distance between them to avoid casting any shadows. The model size is 1.50 m per side with internal measures of 1.35 x 1.35 x 1.35 m, the walls are made up of red brick walls 0.07 x 0.14 x 0.28 m joined and flattened to the outside with cement mortar sand and vinyl paint application. The thickness of these walls is 0.085m with a slab of reinforced concrete 0.07m thick as well as the roof. Finally, the study investigated the design in two seasons hot sub-humid season and hot and humid season.

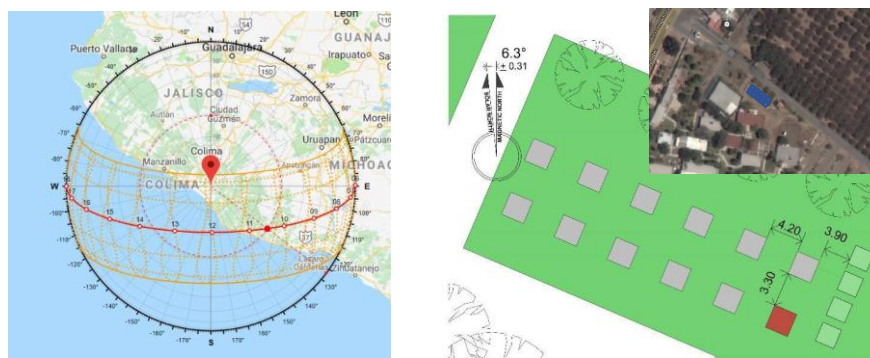


Figure 16: Location of test cells in Coquimatlán.

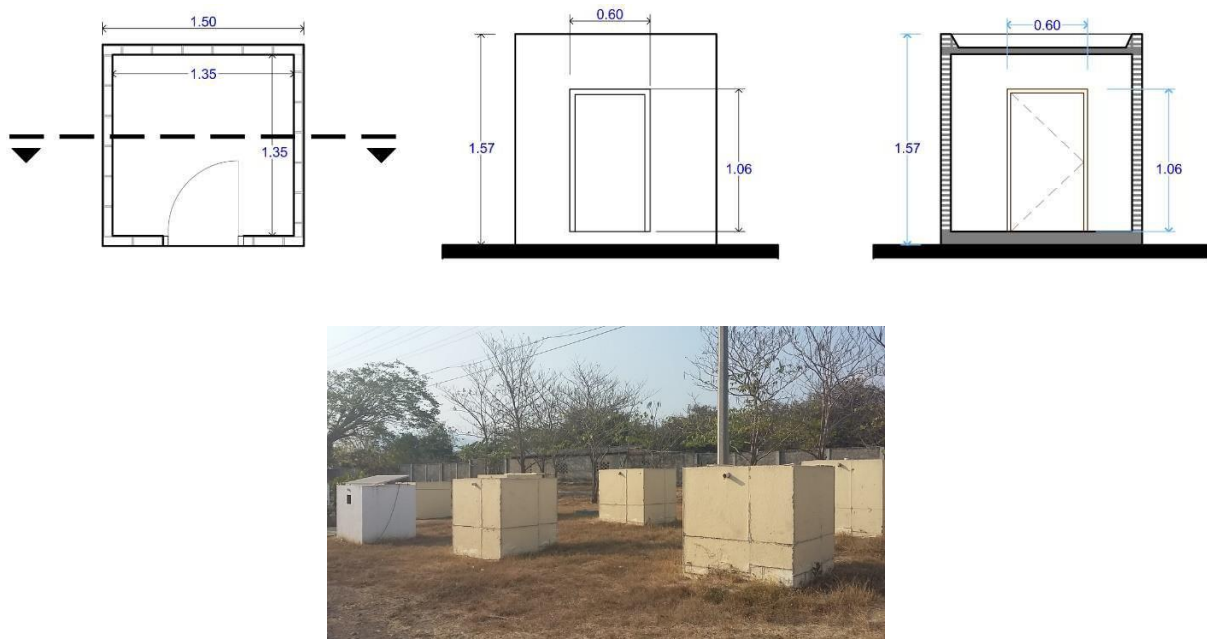


Figure 17: Test cells with details of elevation and cross sections.

The study objective focuses on testing the performance of a device that protects the roof surface from direct solar radiation in the day and allows long-wave radiation at the night as a thermal reduction strategy. The proposal developed a flat radiator system through several configurations to obtain a practical device based on strategies referenced in various investigations (Erell and Etzion, 2000; Frigerio 2004; Bagiorgas et al., 2007; Ghassem et al., 2010; Hollick, 2012; Hanif et al., 2014; Al-Obaidi et al., 2014b; Man, et al., 2015). The research factors developed based on two types of variables: First, independent variables include materials, surface properties, opening, thickness, the gap between surfaces and angle of inclination. Second, dependent variables include dry bulb temperature, mean radiant temperature, wind speed, relative humidity and surface temperature that were obtained from the records of the weather station at the University Centre for Research in Environmental Sciences of the University of Colima (CUICA).

2.3 Characteristics of design models

First, materials and surface properties, it was proposed to assign different materials to determine the best performance for the radiative cooling strategy and subsequently combine different surface properties to achieve an optimum solution. Suitable materials were used in the construction of the proposed device with different thermal properties as Aluminium, Plastic, Metal, Wood and Fiberglass. A flat device of 0.1m thickness was proposed and placed at a height of 0.1m from the parapet as an initial configuration. Second, variations of opening size, the study considered different opening sizes in the device to allow the roof surface to emit radiation to the sky at the night, also the same consideration was taken to prevent receiving direct radiation during the day. These factors were taken with consideration of solar paths during the most critical periods and ensuring the

possibility to achieve the maximum exposure to the sky at night. Third, the cavity between the roof and the device, the design targeted the ventilation strategy to allow the dissipation of the heat that accumulates between the surfaces (Figure 18).

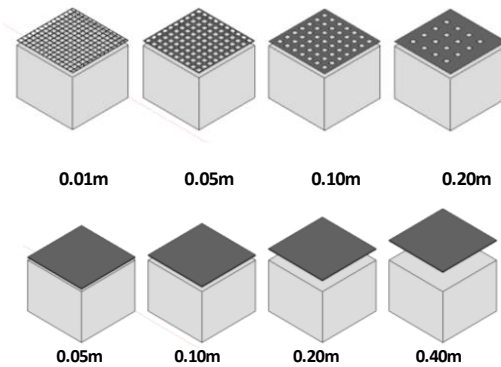


Figure 18: Proposed devices with different opening sizes and cavities dimensions.

The design assessed the opening sizes and device thickness based on solar paths to improve the configurations of vertical elements in the device. The vertical elements were designed to face the south orientation to function as blinds for blocking direct radiation during the day. Specific dates were considered as 21 April/May (equinox) and 21 December/June (solstice). The study found that plotting the geometries of these blinds, a maximum inclination is 45° in April and May, 43° in June and a minimum inclination of 90° in December (Figure 19).

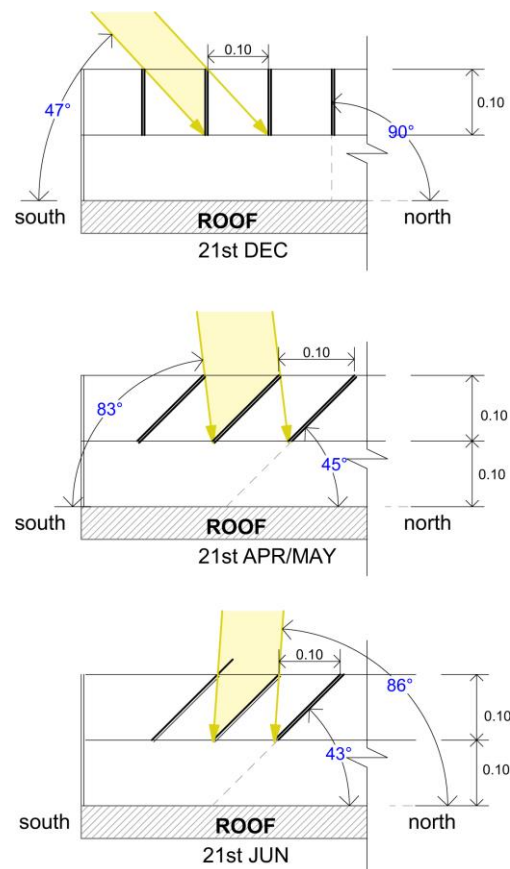


Figure 19: Models of solar blinds in different months.

Based on the assessment of the device geometry, a prototype was developed to meet the environmental requirements. The device was constructed from a wooden frame with the following features: Slatted, multiply and triple wood lattice 1.5m x 1.5m x 0.1m varnished with a grid of 0.10m (Figure 20 and Figure 21). The grid was adjusted at an angle according to the orientation of the experimental models. The device was placed on top of the roof with different heights that ranged between a device on the parapet and a device with a maximum cavity of 0.1m from the roof surface. For the empirical test, the device with blinds of 45° angle was used based on the analysis of solar geometry that protects the roof from most of the direct solar radiation. Two types of air temperatures were recorded, dry-bulb temperature and mean radiant temperature to obtain operative temperatures. Then a comparison between the two records was made to identify the optimum performance.

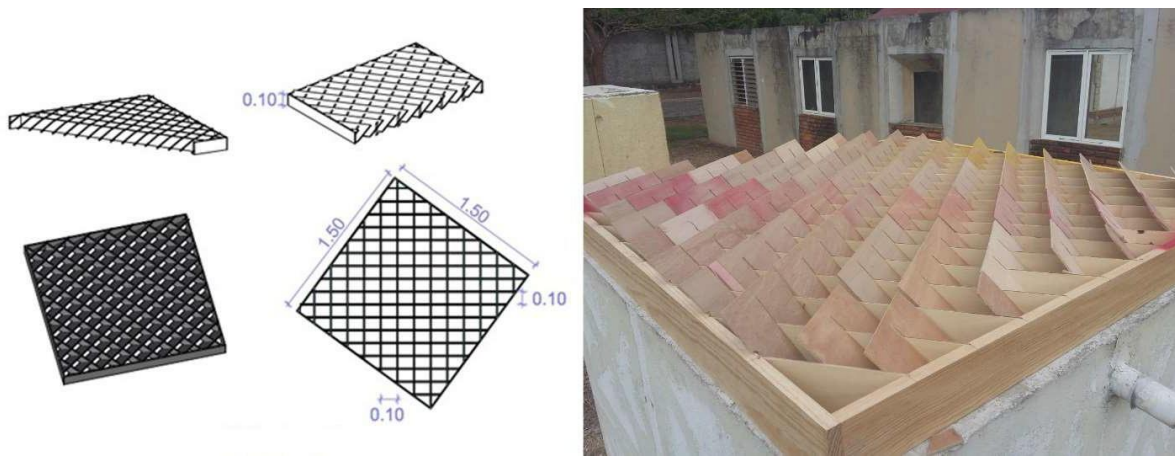


Figure 20: Illustrations of device configurations constructed with pine frame and kumaru plywood boards.



Figure 21: Pictures of the proposed roof device placed on the experimental models attached and separated from the parapet.

2.4 Instruments and equipment

The equipment used in the investigation is listed based on the required elements to be monitored. The interior and exterior surface temperatures of the slab and the walls were tested using Onset models, TMC6-HA connected to datalogger U12-012 and to datalogger H8-004-02. For mean radiant temperature, Onset brand dataloggers model H08- 004-02 were used. For surface temperatures, dry bulb temperature and humidity, Onset brand datalogger model U12-012 was utilised. Monitoring in a semi-controlled environment was carried out prior to the experiment to verify their operation. Table 2 summaries the specifications of the instruments placed in the cells.

Table 2: Specifications of instruments used to monitor test cells.

Device	Description
Onsetcomp models, TMC6-HA	The device accuracy ranges from -40 ° C to 50 ° C in water and -40 ° to 100 ° C in air, accuracy of ± 0.25 ° C from 0 ° to 50 ° C and resolution from 0.03 ° C to 20 ° C. Glued to surfaces using thermal paste and protected by 12 x 12 cm plate of 2" polystyrene.
Dataloggers model H08- 004-02	The device accuracy ranges from -20 ° C to 70 ° C with accuracy of ± 0.4 ° C and resolution of 0.2 ° C.
U12-012 datalogger model	The device accuracy ranges ± 0.35 ° C and between 0 ° C and 50 ° C in temperature and from $\pm 2.5\%$ to 90% in RH. The resolution for the temperature is 0.03 ° C and for the 0.03% RH and both at 25 ° C
HD 2103.1 Delta Ohm	The device accuracy ranges from -5 to 50 ^o C and RH up to 90% without condensation. Also, omnidirectional Delta Ohm AP471S2 hot wire probe with measuring ranges from 0.1 to 5 m/s and from -25 to 80 ° C.

2.5 Instrument calibration

In this research, two types of calibration were carried out, one that refers to the measurement instruments that were used during the monitoring stage of the experimental model and another on the test cell itself. The latter measurement helped to set the guidelines to develop the simulation stage. Statistical corrections of the error by obtaining the correlation of a sample of data under the same climatic conditions was conducted. The study obtained data from the instruments in a specific period under the same conditions that contributed as a reference to graph and model the correlations and trend lines to obtain the equations for the rest of the instruments.

The calibration targeted the preliminary stage of the experiment to monitor indoor air temperatures (dry bulb), black globe temperatures (mean radiant temperature), and surface temperatures. Then a three- dimensional model of the same cell was developed with the help of the Design-Builder software. The simulation model considered the climatic information of the site and properties of the selected materials, in order to validate the outcomes of the virtual model.

An experimental cell was selected for testing as shown in Figure 22, the measurement points were identified, and nomenclature was assigned to detect the position of each sensor with a set of data loggers. In the case of the TMC6-HA sensors due to their cylindrical configuration, they were placed with the use of a thermal paste to provide greater contact with the surface. These sensors were fixed with adhesive tape, and then they were covered with a piece of polystyrene (12 x 12 cm) and fixed with metallic tape.

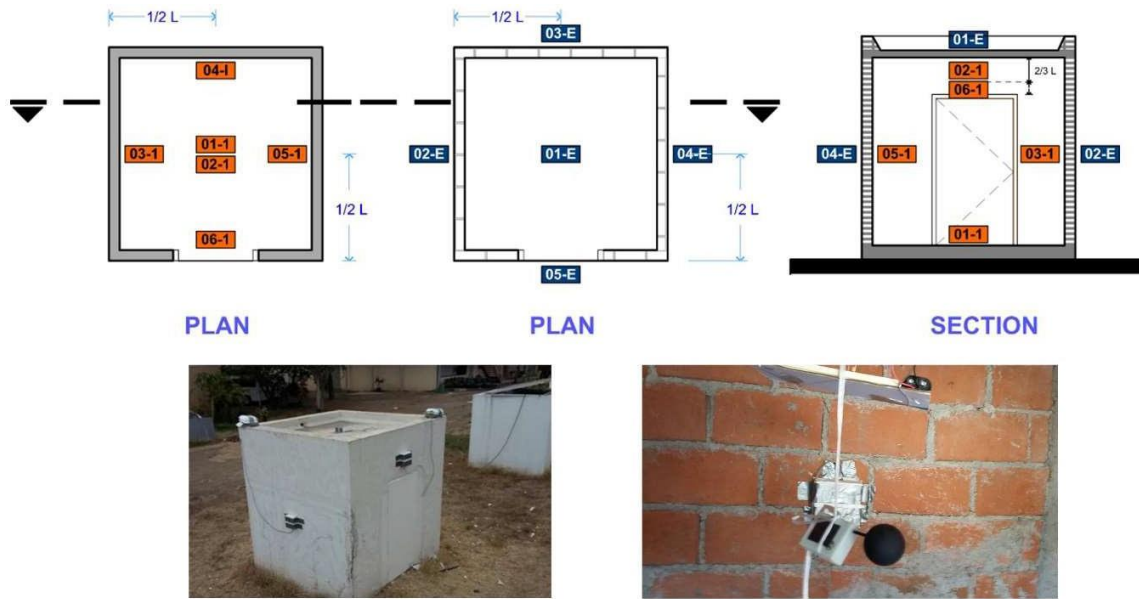


Figure 22: Locations of sensors in the test cell and on its surfaces.

2.6 Simulation and virtual model validation

Design Builder is a software that specializes in environmental and energy simulation of buildings that evaluates comfort levels, energy consumption, ventilation and carbon emissions. Through the Design Builder, a three-dimensional model was developed, replicating the experimental model with the characteristics of materials and the environmental conditions of the site to validate the simulation and CFD calculations. Epw file (EnergyPlus Weather data file) was integrated with the specific meteorological characteristics of the study area. Then a validation of the virtual module was conducted to assess the reliability of simulation outcomes (Shao et al., 2019; Shariati et al., 2019a). The data from equipment placed in the experimental cell was used to generate the operative temperature according to the ASHRAE Standard (ANSI - ASHRAE Standard 55-2017 2017) that was compared to the results obtained by the simulation (Figure 23a). The results of validation showed that outputs from the virtual model have a good agreement with the conditions of the real experimental cell. Two statistical indices were used in the validation, Mean BIAS Error (MBIAS) that measures the difference between two continuous variables and Root Mean Square Error (RMSE), which measures the dispersion of waste. The results showed that RMSE was 0.799 and MBIAS was 0.296 that were considered as acceptable (Ali and Abustan, 2014). Also, a scattered plot was used to identify the correlation coefficient values (r^2) of the simulated data with the observed measurements (Figure 23b). The coefficient for the operative temperature was $r^2=0.9719$ and for the dry bulb temperature was $r^2=0.9535$.

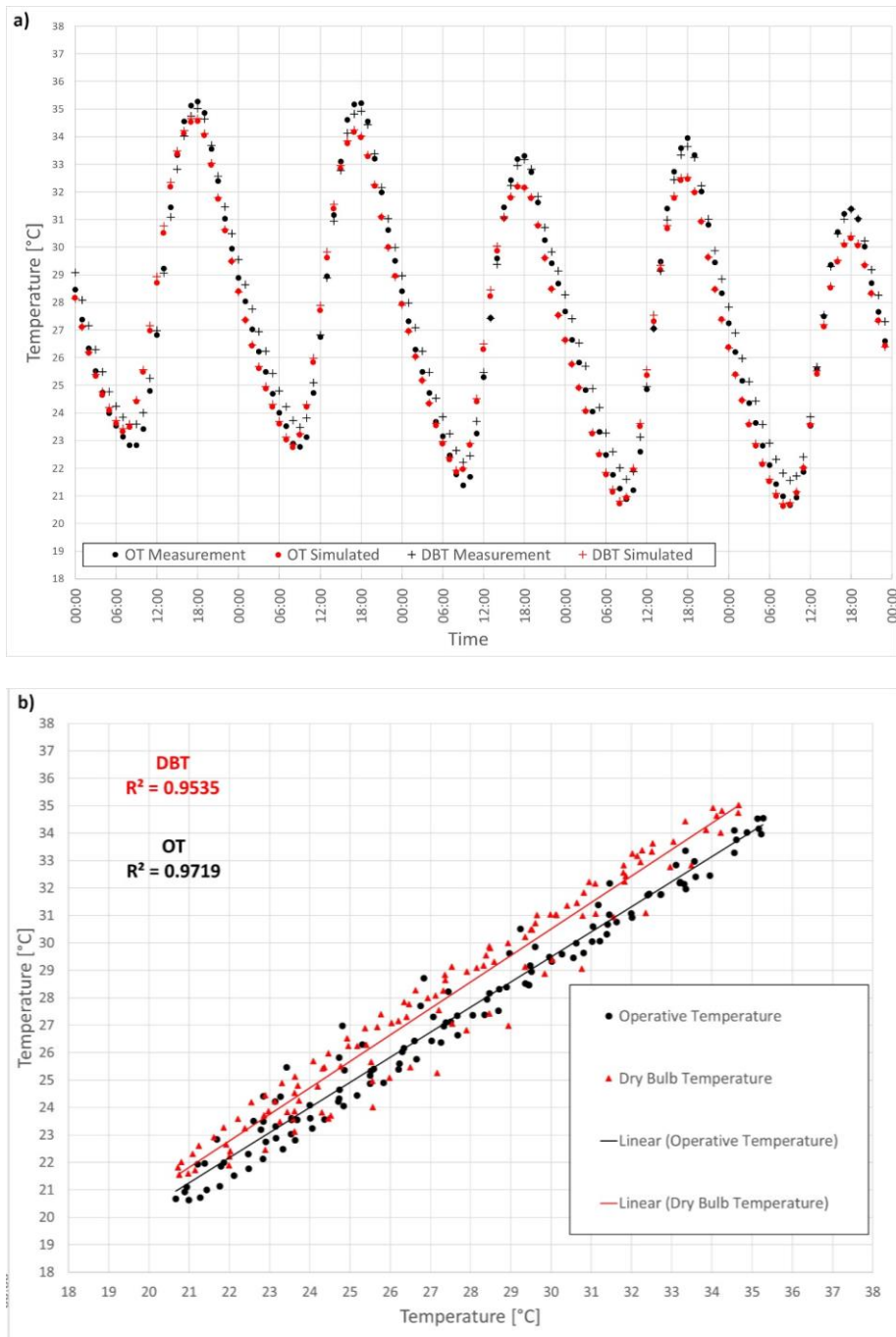


Figure 23: (a) Dry bulb temperatures and operative temperatures in experiment and simulation tests for validation purposes. (b) Regression analysis of dry bulb temperatures and operative temperatures between experiment and simulation tests.

Once the virtual model was determined and validated, design proposals were made to evaluate and analyse their performance. The design proposed to modify the surface properties to control absorptance and emissivity features to improve design performance. Thus, the configurations were set with blinds angles of 43° , 45° and 90° that were painted in white and black then applied for each trial and compared against a reference cell, a full shade cover, and a cool roof cell (Figure 24).

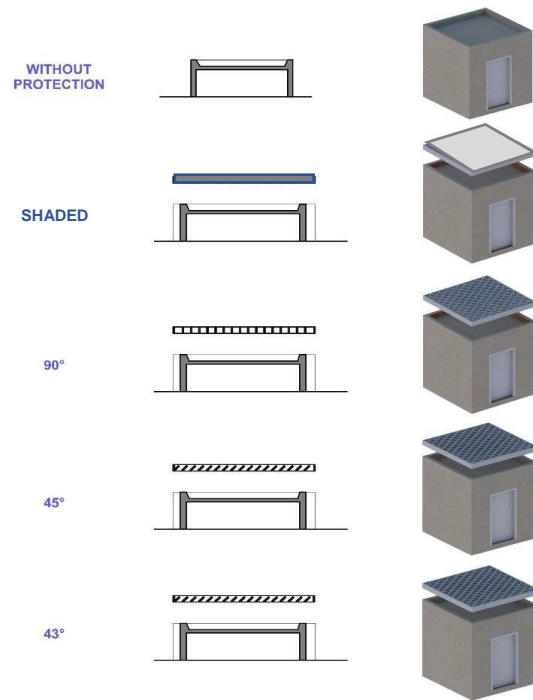


Figure 24: Test models in sections and 3d configurations

3. Results and analysis

The results of the simulations are presented in two parts. The first part shows the findings of the design configurations through the application of different opening size, the cavity size between the proposed device and the roof and the efficiency of blinds with different tilt angles in hot sub-humid and hot and humid seasons. The second part presents the results of the proposed device with different surface properties in both seasons. Finally, the last part discusses the findings of Tukey Test for all the cases with different surface properties in both seasons.

3.1 Design configurations

3.1.1 Performance of the device with different opening sizes

In the first phase, the study assessed the performance of the device with different opening sizes to block the direct solar radiation from reaching the concrete roof (Figure 25). The following percentages were proposed as 20%, 40%, 80% and 88% with opening sizes of 0.20m, 0.10m, 0.05m and 0.01m, respectively.

In the hot sub-humid season, the performance was recorded with different opening sizes in hot days. The representative day was on 21 April, the operative temperatures of openings 20%, 40%, 80% and 88% recorded as the maximum temperatures were 34.9°C, 31.8°C, 30.6°C and 30.0°C, the average temperatures were 30.7°C, 29.2°C, 28.5°C and 28.1°C and the minimum temperatures were 26.8°C, 26.4°C, 26.1°C and 26°C, respectively. The oscillations recorded 8.1°C, 5.5°C, 4.5°C and 4°C, respectively. The differences remain close at night, but during the day, after 9:00, it was observed

that indoor temperatures increased between 16:00 and 17:00. It reached its maximum with the opening of 40% that was approximately 3°C while with the opening of 88% was 5°C (Figure 26).

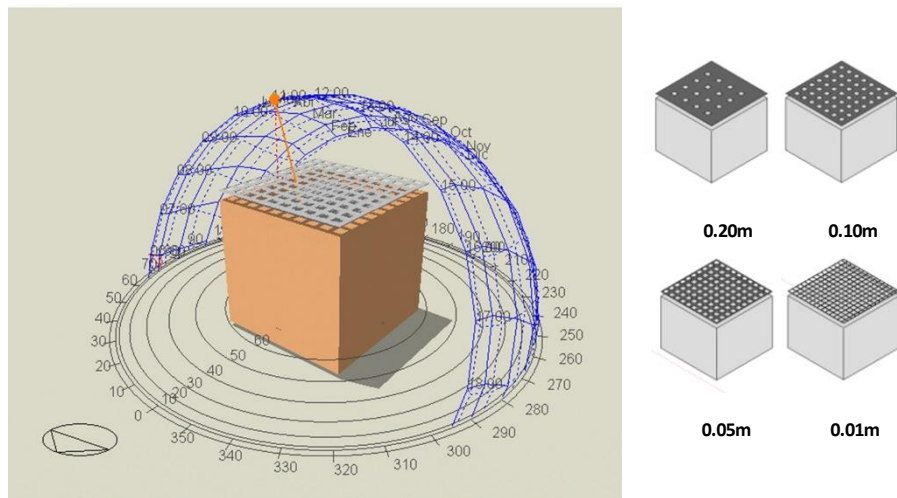


Figure 25: Proposed cover with different opening sizes.

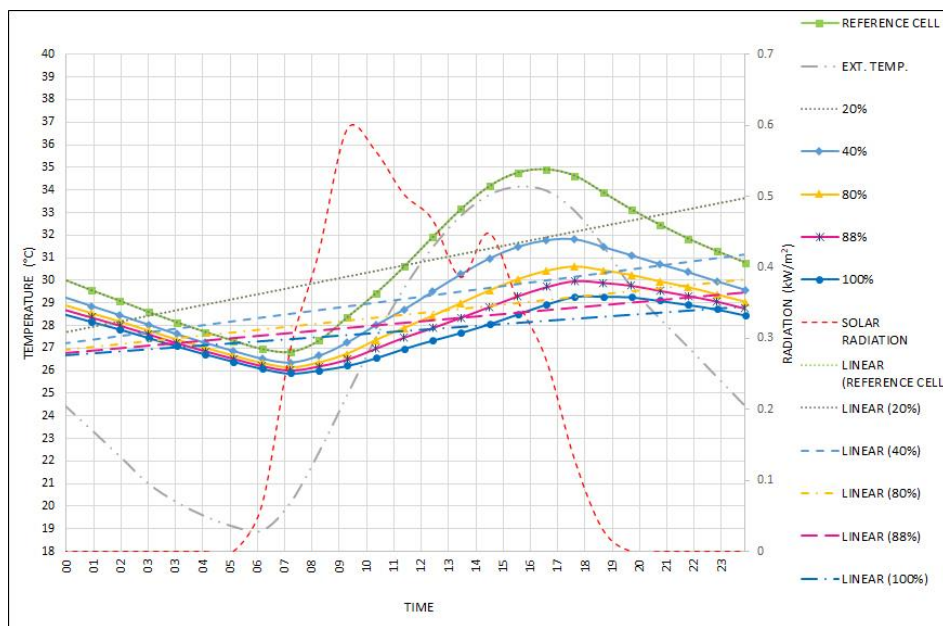


Figure 26: Performance of the device with different openings in a typical day in hot sub-humid season.

The tests of significance were run with the student's t-statistic, the null and alternative hypotheses were stated for its verification.

H0 = There is no significant difference in temperature when applying the device.

H1 = There is a significant difference in temperature when the device is applied.

The t test was used for two samples assuming equal variances, between the variations of openings and the control model. With 20% opening, there was no difference, even the test recorded 0 in the t-statistic. For 40% opening, there was a slight difference in the graph of the t-statistic, but it was insignificant, however, with 88% opening the difference recorded a significant value. Student's t-statistic in device opening variations in hot sub-humid season in the order of 20%, 40%, 80% and 88% were 0, 2.3488035, 3.6008064 and 4.2737148.

In hot and humid season, the performance of openings as shown in Figure 27 did not behave differently from other seasons. The representative day was on 31 August, the operative temperatures of openings 20%, 40%, 80% and 88% recorded as the maximum temperatures were 38.5°C, 35.4°C, 34.1°C and 33.6°C, the average temperatures were 34.6°C, 33.0°C, 32.3°C and 31.9°C and the minimum temperatures were 31.1°C, 30.5°C, 30.3°C and 30.1°C. The oscillations recorded 7.4°C, 4.9°C, 3.8°C and 3.4°C, respectively. Similar to the hot sub-humid season, the differences remain close at night, it was observed that the temperatures increased especially between 16:00 and 17:00. The maximum difference with the opening of 40% was approximately 3°C while with the opening of 88% was 5°C.

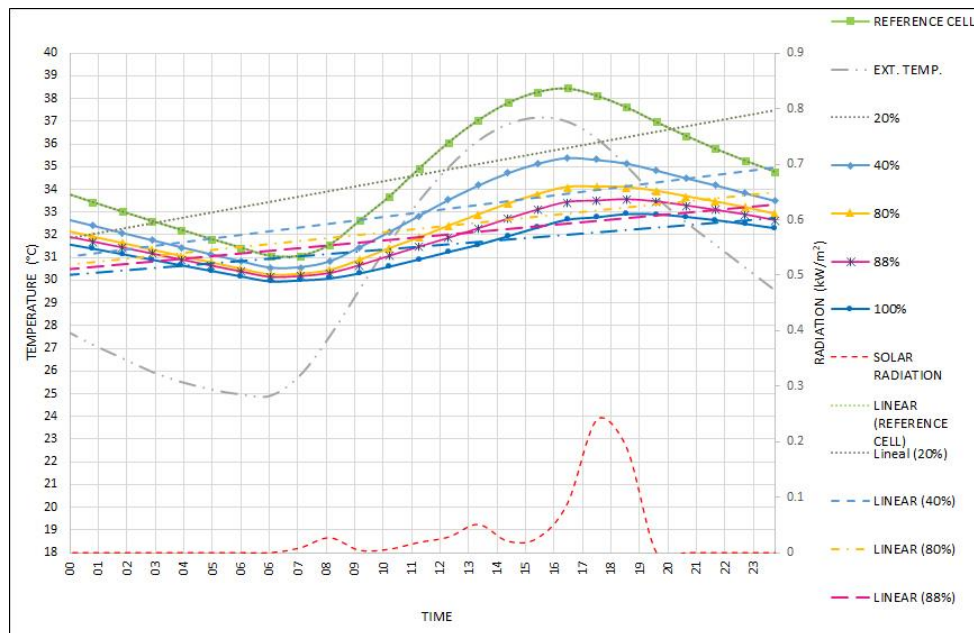


Figure 27: Performance of the device with different openings in a typical day in hot humid season.

The results of significance tests showed that the differences are significantly similar to hot sub-humid season. There was an increase in the t statistic due to the rise in air temperatures. Student's t-statistic in the device with openings in the order of 40%, 80% and 88% were 0, 2.7180359, 4.1662544 and 4.9345926.

3.1.2 Performance of cavity size between the roof and the device

The second phase presents the simulation outcomes that were generated by testing the performance of different cavities between the roof and the device as shown in Figure 28. In the hot sub-humid season, Figure 29 shows the operative temperatures of targeted cavities 0.05m, 0.10m, 0.20m and 0.40m. The maximum temperatures were 29.2°C, 29.3°C, 29.6°C and 30.2°C, the average temperatures were 27.7°C, 27.8°C, 27.9°C and 28.2°C, the minimum temperatures were 25.9°C, 25.9°C, 25.9°C and 26.3°C, respectively. The oscillations recorded 3.6°C, 3.4°C, 3.7°C and 4.2°C, respectively.

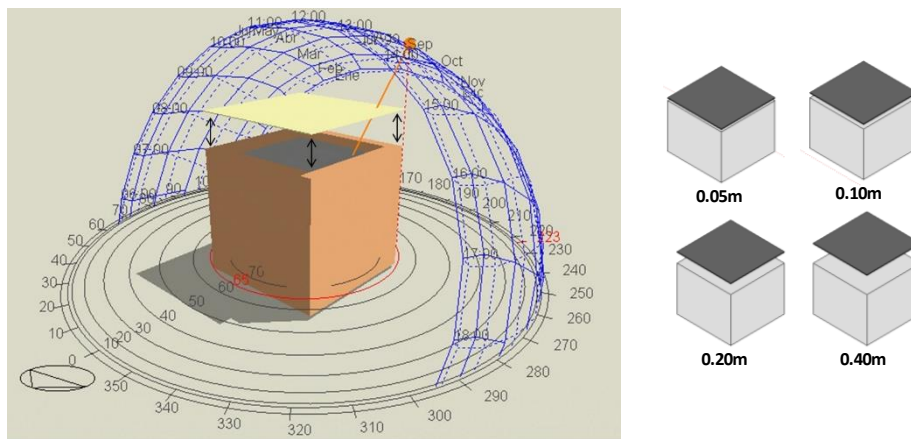


Figure 28: Proposed cover with different cavities.

In this season the t-statistic shows improved performance and an increase in the significant differences. Student's t-statistic in the order of 0.05 m, 0.10 m, 0.20 m and 0.40 m were 5.0803937, 4.9940183, 4.7935563 and 4.2026996. The results showed that 0.05m achieved 5.08 compared to 0.40m which recorded 4.20.

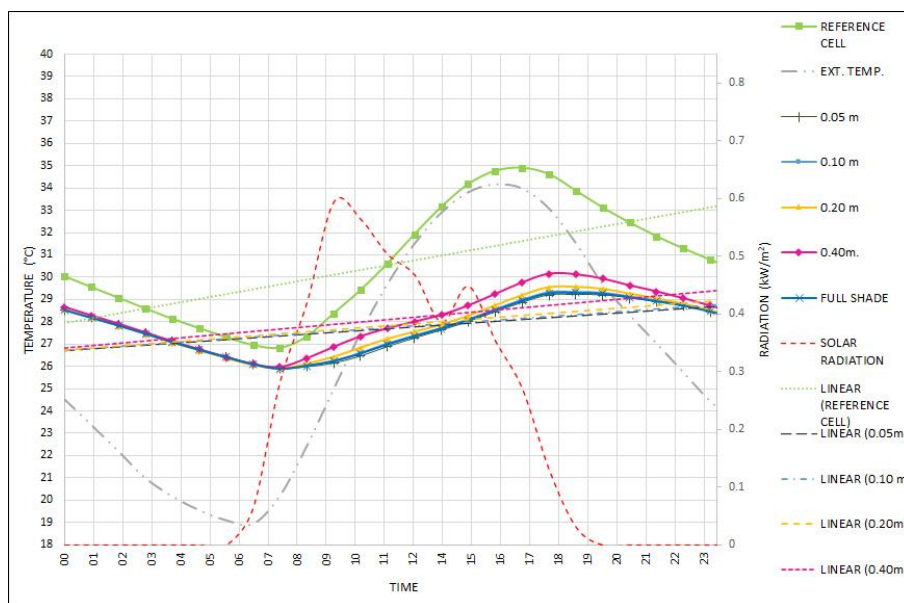


Figure 29: Performance of the device with different cavities in hot sub-humid season.

In hot and humid season, Figure 30 shows the performance of operative temperatures in the proposed cavities 0.05m, 0.10m, 0.20m. and 0.40m. In the same order, the maximum temperatures were 32.8°C, 32.9°C, 33.2°C and 33.8°C, the average temperatures 31.4°C, 31.5°C, 31.6°C and 32°C, at minimum temperatures 30°C, 30°C, 30°C and 30.1°C, respectively. The oscillations recorded 2.9°C, 3°C, 3.2°C and 3.7°C, respectively. This season shows another increase in significant differences, Student's t-statistic with different cavities in the order of 0.05m, 0.10m, 0.20m and 0.40m were 5.9566549, 5.7997276, 5.4836271 and 4.7324692. The results showed that 0.05m achieved 5.95 compared to 0.4m which recorded 4.73.

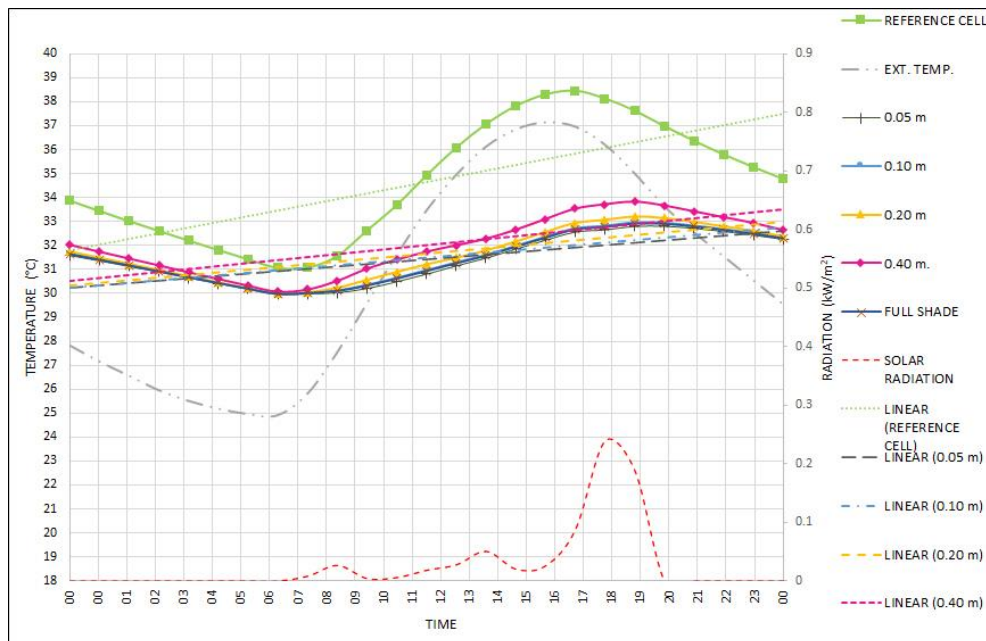
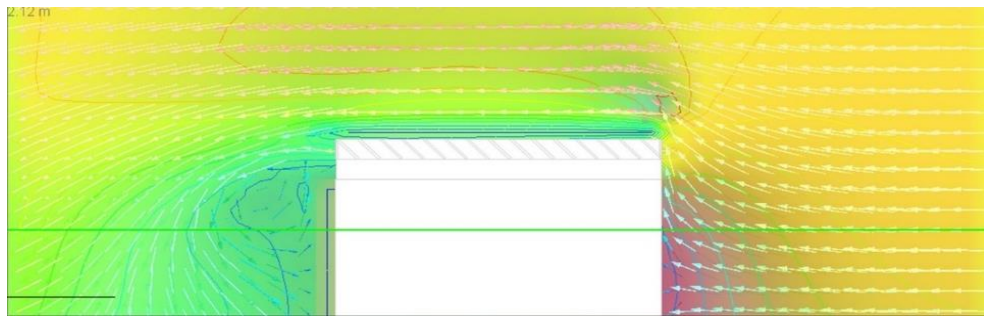
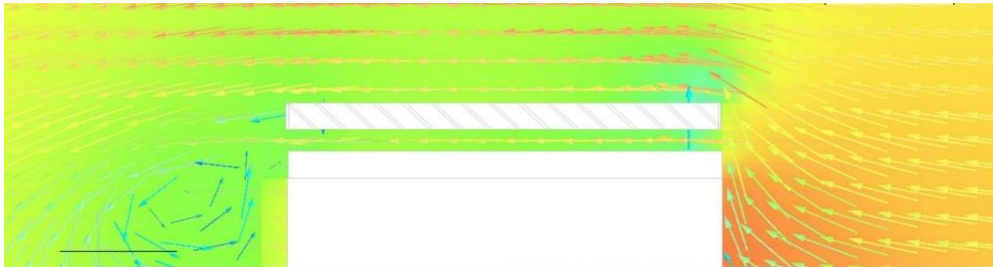


Figure 30: Performance of the device with different cavities in hot and humid season.

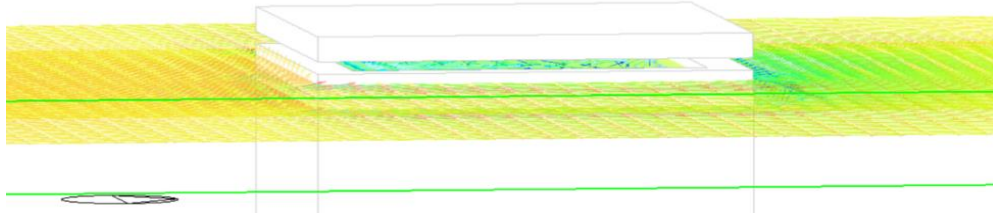
Further examination was conducted through Computational Fluid Dynamics (CFD) using DesignBuilder CFD analysis to assess the effectiveness of the cavity between the roof and the device. Figure 31 shows the device with two cavities 0.10m and 0.05m. The analysis of 0.10m revealed the speed of airflow between the roof and the device, the analysis showed an equivalent air speed to the outside. This indicates that the space under the device is practically exposed to a convective exchange with the outside air. However, by placing the device nearer to the surface of the roof with height 0.05m, the speed of airflow dropped in the contained space and it was no longer equal to the outside, but the airflow started to move slowly in all directions. In fact, this airflow behaviour would help to maintain the contained air for a longer period which boosts the cooling effect when the air is shaded. However, in the opposite case when the cavity was increased, the roof was exposed to the outdoor environment and the device efficiency dropped as a blocker to minimise heat from the outside air.



CFD analysis of the device attached on the roof with no cavity.



CFD analysis of the device with 0.10m cavity.



CFD analysis of the device with 0.05m cavity.



Figure 31: CFD analysis of the device with different cavities.

3.1.3 Performance of the device with blinds and different tilt angles

Figure 32 and Figure 33 present the outcomes of different tilt angles of the blinds in the proposed device compared to a reference cell, a full shade device and a cool roof strategy. Figure 32 shows the results of the hot sub-humid season, the analysis indicated that the thermal swing is higher compared to other seasons. The analysis showed that operative temperatures with different tilt angles have higher readings compared to a reference cell, a full shade device, and a cool roof cell. However, trend lines indicate that the performance of all cases is similar. Figure 33 shows the results

of the hot humid season, the outcomes of thermal swing was found to be lower than the sub-humid season due to the humidity in the air in this season. The readings of full shade (red colour) presented the lowest thermal swing compared to all experimental cells. Nevertheless, as observed in trend lines, the reference cell, cool roof and tilt angle 90° recorded the highest operative temperatures. To identify the differences in each case, Tukey All-Pairwise Comparisons test was used. Table 3 shows that all proposed tilt angles have similar performance as the reference cell. The main difference remains in the maximum and the minimum values. The analysis of maximum temperatures showed that devices with full shade and cool roof configurations were found to be the lowest at midday, however, the two configurations recorded the highest in the minimum temperatures at early morning.

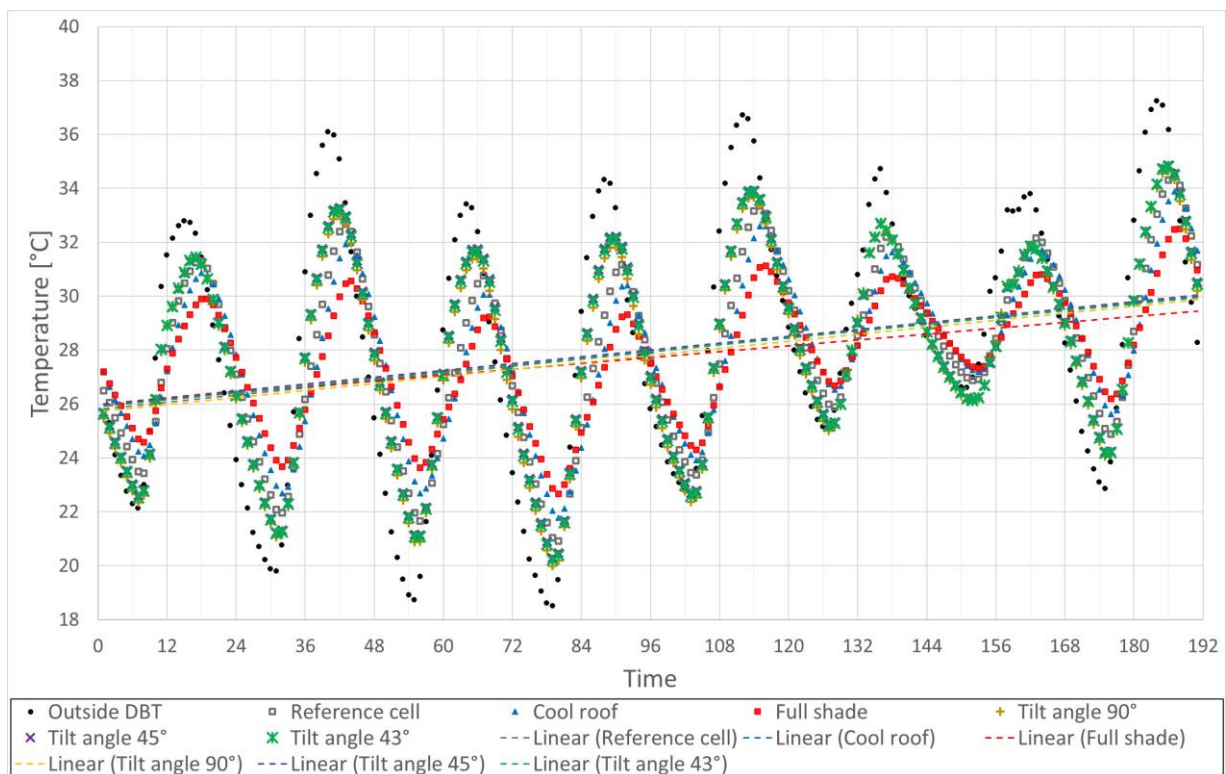


Figure 32: Thermal behaviour of test cells with different configurations in the hot sub-humid season.

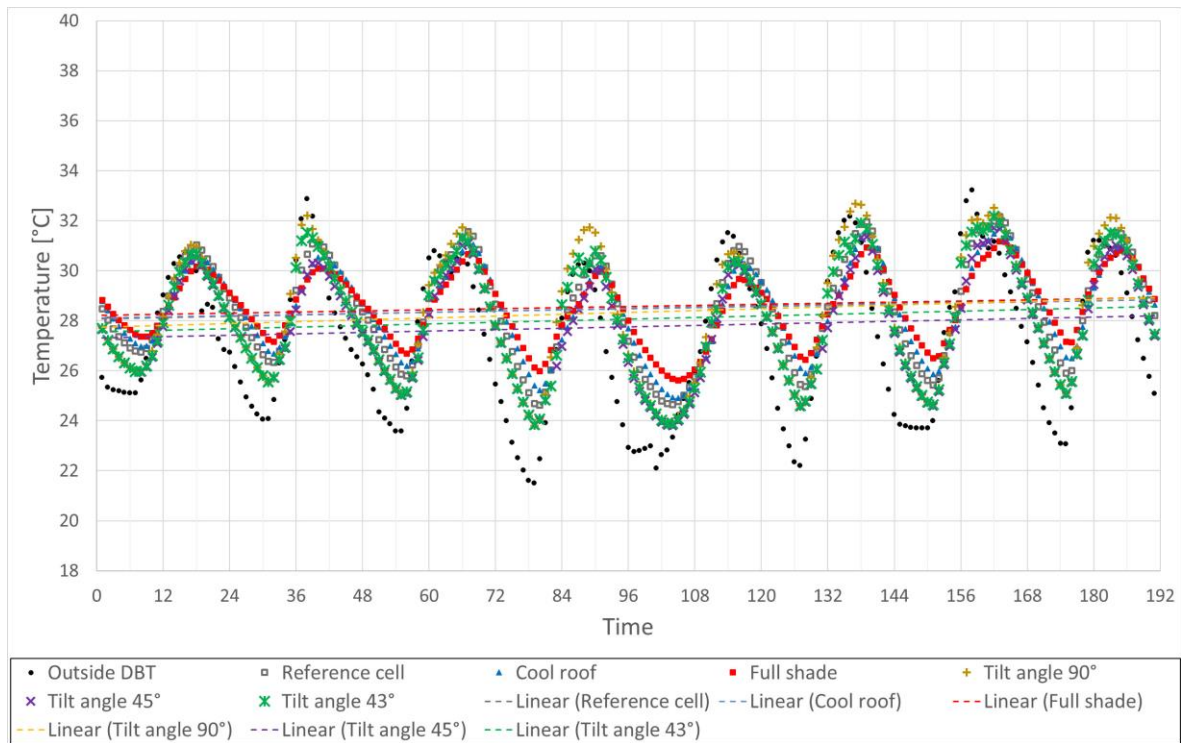


Figure 33: Thermal behaviour of test cells with different configurations in the hot humid season.

Table 3: Tukey test for all the cases in hot sub humid and hot and humid seasons.

	Mean values		
	Case	Mean	Homogeneous Groups
Hot Sub-Humid	Full shade	28.57	A
	Reference	28.50	A
	Cool roof	28.47	A
	Tilt 90	28.33	A
	Tilt 43	28.08	AB
	Tilt 45	27.75	AB
	Outside DB	27.20	B
Hot Humid	Full shade	28.57	A
	Reference	28.50	A
	Cool roof	28.47	A
	Tilt 90	28.33	A
	Tilt 43	28.08	AB
	Tilt 45	27.75	AB
	Outside DB	27.20	B
	Alpha	0.05	Standard Error for Comparison 0.3209
	Critical Q Value	4.346	Critical Value for Comparison 0.9861

3.2 Performance of different surface properties

Figure 34 and Figure 35 show the analysis of devices with different colours and configurations in hot sub-humid and hot and humid seasons. The thermal behaviour of the full shade device showed a lower increment in temperatures during the day due to the capability of the device to block direct solar radiation. However, during the period of low temperature, the analysis showed that the device was incapable to allow radiative cooling which reduces its efficiency during the night and early morning periods. In the case of the proposed devices with different tilt angles 43°, 45°, and 90° both in white and in black colours, the readings presented similar performance during the night, however, during the day a difference can be observed with a device of 90° in black that performed better than other models.

To improve the reliability of outcomes for each type of roof cover, the trend lines were investigated in the graphs for each type. The differences between the cases were noticeable in minimum and maximum temperatures but in mean temperatures, the performance was alike. To identify the significant difference between the mean temperatures of all cases without modification in the surface properties, a Tukey test was used, and a statistic test was conducted as shown in Table 4.

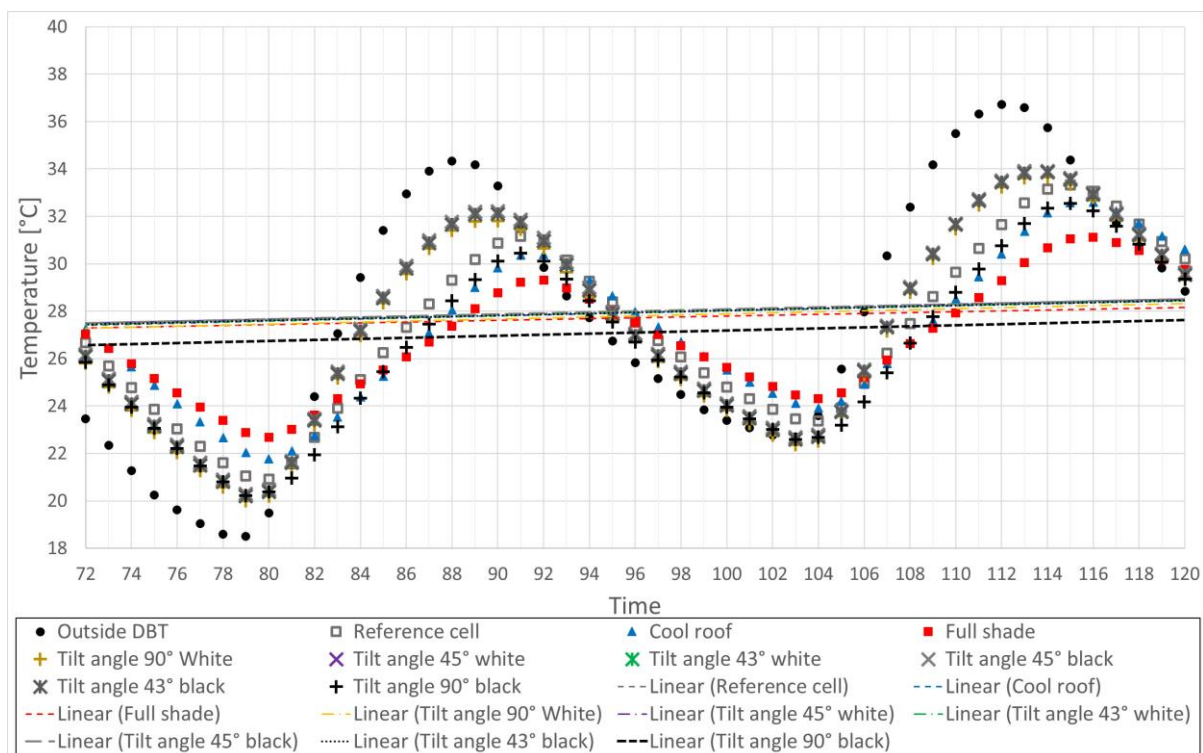


Figure 34: Thermal behaviour of test cells with different colours and configurations in hot sub-humid season.

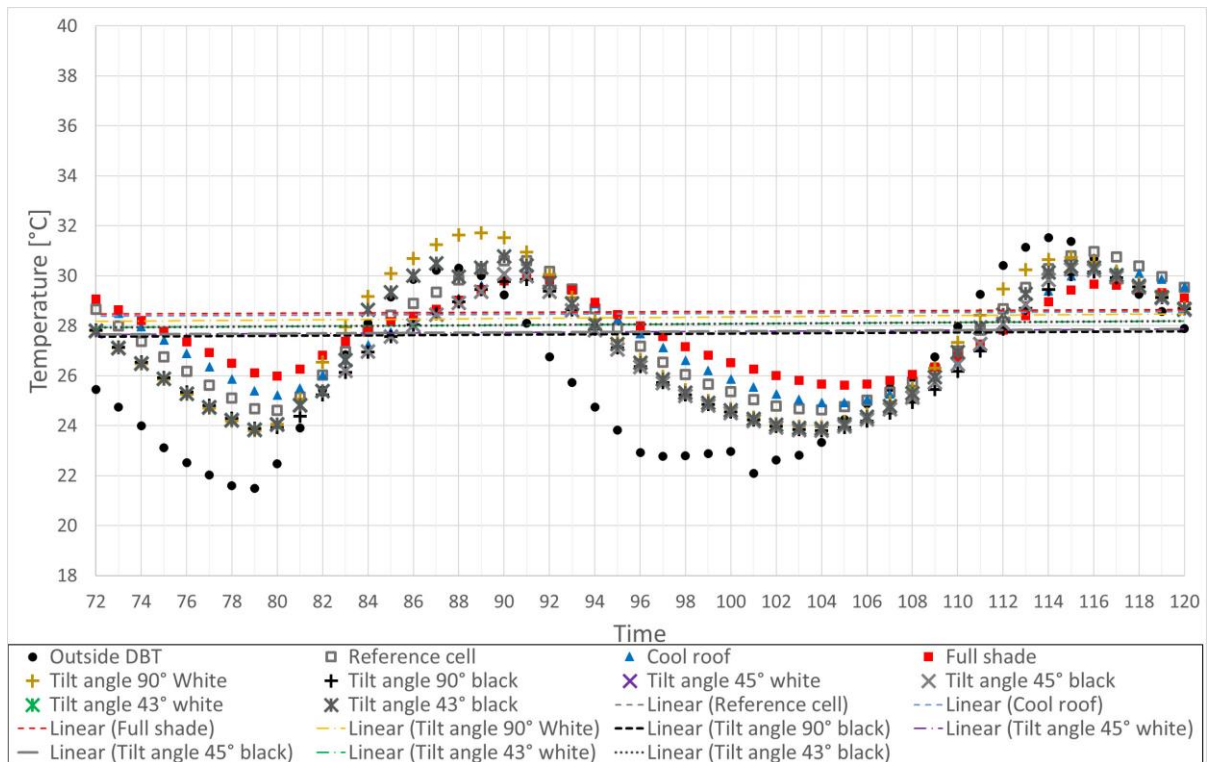


Figure 35: Thermal behaviour of test cells with different colours and configurations in hot and humid season.

Table 4: Tukey test of devices with different colours in hot sub-humid and hot and humid seasons.

		Mean values		
		Case	Mean	Homogeneous Groups
Hot and Humid	Black	Full shade	28.57	A
		Reference	28.50	A
		Cool roof	28.47	A
		Tilt 43	28.08	AB
		Tilt 45	27.75	AB
		Tilt 90	27.67	AB
		Outside DB	27.20	B
	White	Full shade	28.57	A
		Reference	28.50	A
		Cool roof	28.47	A
		Tilt 90	28.33	A
		Tilt 43	28.08	AB
		Tilt 45	27.75	AB
		Outside DB	27.20	B

Hot Sub-Humid	Black	Outside DB	28.24	A
		Tilt 45	28.01	AB
		Cool roof	27.96	AB
		Tilt 43	27.95	AB
		Reference	27.94	AB
		Full shade	27.73	AB
		Tilt 90	27.11	B
	White	Outside DB	28.24	A
		Tilt 45	28.01	A
		Cool roof	27.96	A
		Tilt 43	27.95	A
		Reference	27.94	A
		Tilt 90	27.80	A
		Full shade	27.73	A
	Alpha	0.05	Standard Error for Comparison 0.3187	
	Critical Q Value	4.81	Critical Value for Comparison 1.0838	

Table 4 shows a significant difference in the mean value of operative temperature between the device with blinds of 90° in black and the outside air temperature in the hot sub-humid season. This indicates that the device managed to achieve low temperatures compared to other models, however, the performance of other devices was insignificant. In the hot humid season, the analysis of devices with different surface properties showed insignificant differences, but the full shade, reference cell and cool roof and the 90° tilt in white have higher temperatures compared to other models. In the hot sub-humid season, the results of the full shade cover recorded a short swing, but the trend line showed an average temperature that is higher compared to other test cells. In the devices with tilt angles 43°, 45° and 90°, the analysis identified two groups, group 1 includes 90° Black, 45° White and 45° Black while group 2 includes 90° White, 43° White and 43° Black. The outcomes of two groups indicated that group 1 managed to be cooler 1°C - 2°C than group 2. This difference begins to diminish as the temperature falls at 20:00. The performance of the first group showed that the roof surface has a higher exposure to the sky compared to the second group. Although the roof with a device of 90° is exposed to the sky during the day, the absorbance of solar radiation was affected by the reflective and convective effect in white and black colours.

4. Conclusion

This research presented a study that assessed the performance of a passive device on a flat concrete roof in the state of Colima, Mexico. A prototype is introduced as a passive device installed on an existing roof, potentially walkable, and compatible with the operation of the existing roofs to meet the objectives of this study. The device acts as a protective element to block direct solar radiation and at the same time allow cooling by emitting longwave radiation during the night. The results of empirical investigation and simulation tests were recorded to identify the optimum configuration.

The performance of a perforated device with different configurations was investigated. The results showed that a device with an opening percentage of 88% with a cavity of 0.05m between the roof and the device provided effective protection. The study found that the proposed device with different thicknesses has no effect on operative temperatures as heat conduction process was not

performed between the roof and the device in the investigation. Furthermore, the device with blinds of 45° recorded lower operative temperatures within a range of mean values between 0.8°C and 0.9°C compared to a roof with full shade cover in the hot and humid season. However, the perforated device with blinds of 90° in black colour delivered the best performance compared to other models and recorded a mean value of 1.13°C in the hot sub-humid season. Further investigations showed that applying white waterproofing onto the roof was noticeable, the data recorded lower operative temperature with 0.39°C in hot sub-humid and 0.34°C in hot and humid season. As a result, the study found that perforated devices show an increase in night cooling compared to a full shade device on top of flat roofs in western Mexico.

References

- Acosta, J., Aguilar, G. (2018). The green mortgage program of INFONAVIT: towards a sustainable housing policy? *Vivienda y comunidades sustentables*, 2(3), 25-34.
- Ali, M. H., & Abustan, I. (2014). A new novel index for evaluating model performance. *Journal of Natural Resources and Development*, 4, 1-9.
- Almodovar, J. M., & La Roche, P. (2019). Roof ponds combined with a water-to-air heat exchanger as a passive cooling system: Experimental comparison of two system variants. *Renewable energy*, 141, 195-208.
- Al-Obaidi, K. M., Ismail, M., & Rahman, A. M. A. (2014a). Passive cooling techniques through reflective and radiative roofs in tropical houses in Southeast Asia: A literature review. *Frontiers of Architectural Research*, 3(3), 283-297.
- Al-Obaidi, K. M., Ismail, M., & Rahman, A. M. A. (2014b). Design and performance of a novel innovative roofing system for tropical landed houses. *Energy conversion and management*, 85, 488-504.
- Al-Obaidi, K. M., Ismail, M., & Rahman, A. M. A. (2014c). Investigation of passive design techniques for pitched roof systems in the tropical region. *Modern Applied Science*, 8(3), 182.
- Al-Obaidi, K. M., Ismail, M. A., & Abdul Rahman, A. M. (2016). Effective use of hybrid turbine ventilator to improve thermal performance in Malaysian tropical houses. *Building Services Engineering Research and Technology*, 37(6), 755-768.
- Bahadori, M. N., Dehghani-Sanij, A., & Sayigh, A. (2014). *Wind towers: architecture, climate and sustainability*. Springer.
- Bagiorgas, H. S., & Mihalakakou, G. (2008). Experimental and theoretical investigation of a nocturnal radiator for space cooling. *Renewable Energy*, 33(6), 1220-1227.
- Bosi, S. G., Bathgate, S. N., & Mills, D. R. (2014). At last! A durable convection cover for atmospheric window radiative cooling applications. *Energy Procedia*, 57, 1997-2004.
- Dimoudi, A., & Androutsopoulos, A. (2006). The cooling performance of a radiator based roof component. *Solar energy*, 80(8), 1039-1047.

Duarte, H. F., Dias, N. L., & Maggiotto, S. R. (2006). Assessing daytime downward longwave radiation estimates for clear and cloudy skies in Southern Brazil. *Agricultural and forest meteorology*, 139(3-4), 171-181.

D'Orazio, M., Di Perna, C., & Di Giuseppe, E. (2010). The effects of roof covering on the thermal performance of highly insulated roofs in Mediterranean climates. *Energy and Buildings*, 42(10), 1619-1627.

Erell, E., & Etzion, Y. (2000). Radiative cooling of buildings with flat-plate solar collectors. *Building and environment*, 35(4), 297-305.

El Bachawati, M., Manneh, R., Belarbi, R., Dandres, T., Nassab, C., & El Zakhem, H. (2016). Cradle-to-gate Life Cycle Assessment of traditional gravel ballasted, white reflective, and vegetative roofs: A Lebanese case study. *Journal of Cleaner Production*, 137, 833-842.

Esparza-López Carlos J. (2015) Estudio experimental de dispositivos de enfriamiento evaporativo indirecto para un clima cálido subhúmedo. *Tesis de Doctorado. Universidad de Colima. Facultad de Arquitectura y Diseño. Colima.*

Esparza, C., del Pozo, C. E., Gómez, A., Gómez, G., & Gonzalez, E. (2018). Potential of a wet fabric device as a roof evaporative cooling solution: Mathematical and experimental analysis. *Journal of Building Engineering*, 19, 366-375.

Feng, W., Zhang, Q., Ji, H., Wang, R., Zhou, N., Ye, Q., ... & Lau, S. S. Y. (2019). A review of net zero energy buildings in hot and humid climates: Experience learned from 34 case study buildings. *Renewable and Sustainable Energy Reviews*, 114, 109303.

Frayssinet, L., Merlier, L., Kuznik, F., Hubert, J. L., Milliez, M., & Roux, J. J. (2018). Modeling the heating and cooling energy demand of urban buildings at city scale. *Renewable and Sustainable Energy Reviews*, 81, 2318-2327.

Frigerio, E. (2004). Radiación nocturna: campanas en Cachi. *Avances en Energías Renovables y Medio Ambiente*, 8.

Givoni Baruch, (1977) Solar Heating and Night Radiation Cooling by a Roof Radiation Trap. *Energy and Building* 1(1977) 141-145.

Gómez Azpeitia Gabriel, Cruz Sara, Gómez Adolfo, Alcántara Armando, (2005) *El entorno arquitectónico como factor asociado a la violencia doméstica en Colima*, Iridia de la Universidad de Colima, Año 1 número 02.

González, E. (1997). Técnicas de enfriamiento pasivo. Resultados experimentales en el clima cálido y húmedo de Maracaibo, Venezuela. *CIT, Información Tecnológica*, 8(5), 99-103.

González, E. (2002). Enfriamiento radiativo en edificaciones. *Notas del Curso de actualización.*

González, M. (2011). Comportamiento de dos dispositivos de ventilación por extracción pasiva en un clima cálido subhúmedo. *Tesis de maestría no publicada. Universidad de Colima. Facultad de Arquitectura y Diseño. Colima.*

González-Cruz, E. M., & González-García, S. I. (2013). Estudio experimental sobre el comportamiento térmico de un nuevo tipo de techo-estanque para el enfriamiento pasivo en clima húmedo. *Ambiente Construido*, 13(4), 149-171.

González-Yñigo, M., Méndez-Ramírez, J. (2018). The sustainable housing policy in Mexico product of the transformations of the welfare state to the neo-liberalism state. Case of the National Housing Fund for the Worker 2006-2015. *Quivera. Revista de estudios territoriales*, 20(1), 71-84.

Guarneros Urbina Laura I., Velasco Sandoval Alberth F. (2012) Eficiencia, Accesibilidad y Componentes de los Sistemas de Enfriamiento Natural en Regiones Cálido Húmedo. *Revista ARCUS Año 2 No. 2 pag.40-46*. Facultad de Arte y Diseño de la Institución Universitaria Colegio Mayor del Cauca. http://www.colmayorcauca.edu.co/web/uploads/revista_arcus_2012_Full.pdf

Hanif, M., Mahlia, T. M. I., Zare, A., Saksahdan, T. J., & Metselaar, H. S. C. (2014). Potential energy savings by radiative cooling system for a building in tropical climate. *Renewable and sustainable energy reviews*, 32, 642-650.

Hay, H., & Yellott, J. (1969). Natural air conditioning with roof ponds and movable insulation. *ASHRAE Trans.;(United States)*, 75.

Heidarinejad, G., Farahani, M. F., & Delfani, S. (2010). Investigation of a hybrid system of nocturnal radiative cooling and direct evaporative cooling. *Building and Environment*, 45(6), 1521-1528.

Herrera, L. (2009). *Evaluación de estrategias bioclimáticas aplicadas en edificios y su impacto en la reducción del consumo de agua en equipos de enfriamiento evaporativo directo* (Doctoral dissertation, Tesis de Doctorado publicada. Universidad de Colima, Facultad de Arquitectura, Coquimatlán).

Hollick, J. (2012). Nocturnal radiation cooling tests. *Energy Procedia*, 30, 930-936.

Imran, H. M., Kala, J., Ng, A. W. M., & Muthukumaran, S. (2018). Effectiveness of green and cool roofs in mitigating urban heat island effects during a heatwave event in the city of Melbourne in southeast Australia. *Journal of Cleaner Production*, 197, 393-405.

Kimball, B. A. (1985). Cooling performance and efficiency of night sky radiators. *Solar energy*, 34(1), 19-33.

Lechner, N. (2014). *Heating, cooling, lighting: Sustainable design methods for architects*. John Wiley & Sons.

Li, H., & Wang, S. (2020). Coordinated robust optimal design of building envelope and energy systems for zero/low energy buildings considering uncertainties. *Applied Energy*, 265, 114779.

Man, Y., Yang, H., Qu, Y., & Fang, Z. (2015). A novel nocturnal cooling radiator used for supplemental heat sink of active cooling system. *Procedia Engineering*, 121, 300-308.

Martinez-Torres, K., Alcántara, A., Bojórquez, G., Gómez-Azpeitia, L. (2017). Thermal sensation and preference in naturally ventilated dwellings. Manzanillo, Colima. *Cuadernos de arquitectura*, 07(07), 87-97.

McNeil, M., Castellanos, S., de León Barido, P., & Diego Sánchez Pérez, P. A. (2018). Mexico Space Cooling Electricity Impacts and Mitigation Strategies. Analysis Supporting the Summit on Space Cooling Research Needs and Opportunities in Mexico February 15-16 Casa de la Universidad de California, Mexico City. http://cemiegeo.org/images/noticias/mexico_cooling_fact_book-usaid_lbnl.pdf

Mihalakakou, G., Ferrante, A., & Lewis, J. O. (1998). The cooling potential of a metallic nocturnal radiator. *Energy and buildings*, 28(3), 251-256.

Nahar, N. M., Sharma, P., & Purohit, M. M. (2003). Performance of different passive techniques for cooling of buildings in arid regions. *Building and Environment*, 38(1), 109-116.

National Housing Commission. (2015). Programa Nacional de Desarrollo Urbano. <https://www.gob.mx/conavi>

National Institute of Ecology and Climate Change (INECC). (2015). National Inventory of Greenhouse Gas and Greenhouse Gas Emissions 2019. <https://www.gob.mx/inecc/acciones-y-programas/inventario-nacional-de-emisiones-de-gases-y-compuestos-de-efecto-invernadero>

National Institute of Geography and Informatics Statistics (INEGI). (2015). Mexico Intercensal Survey. <http://ghdx.healthdata.org/record/mexico-intercensal-survey-2015>

Nwaigwe, K., Okoronkwo, C. A., Ogueke, N. V., & Anyanwu, E. E. (2010). Review of nocturnal cooling systems. *International Journal of Energy for a Clean Environment*, 11(1-4).

Orel, B., Gunde, M. K., & Krainer, A. (1993). Radiative cooling efficiency of white pigmented paints. *Solar Energy*, 50(6), 477-482.

Parker, D. S. (2005). Theoretical evaluation of the night cool nocturnal radiation cooling concept. *Submitted to: US Department of Energy. FSEC-CR-1502-05.*

Pisello, A. L., Piselli, C., & Cotana, F. (2015). Thermal-physics and energy performance of an innovative green roof system: The Cool-Green Roof. *Solar Energy*, 116, 337-356.

Raman, A. P., Anoma, M. A., Zhu, L., Rephaeli, E., & Fan, S. (2014). Passive radiative cooling below ambient air temperature under direct sunlight. *Nature*, 515(7528), 540-544.

Rahman, A. M. A., & Al-Obaidi, K. M. (2019). *Climate Conscious Low-Energy Tropical Built Environment (Penerbit USM)*. Penerbit USM.

Sabzi, D., Haseli, P., Jafarian, M., Karimi, G., & Taheri, M. (2015). Investigation of cooling load reduction in buildings by passive cooling options applied on roof. *Energy and Buildings*, 109, 135-142.

Schabbach, L. M., Marinoski, D. L., Güths, S., Bernardin, A. M., & Fredel, M. C. (2018). Pigmented glazed ceramic roof tiles in Brazil: Thermal and optical properties related to solar reflectance index. *Solar Energy*, 159, 113-124.

Shao, Z., Gholamalizadeh, E., Boghosian, A., Askarian, B., & Liu, Z. (2019). The chiller's electricity consumption simulation by considering the demand response program in power system. *Applied Thermal Engineering*, 149, 1114-1124.

Shao, Z., Wakil, K., Usak, M., Heidari, M. A., Wang, B., & Simoes, R. (2018). Kriging Empirical Mode Decomposition via support vector machine learning technique for autonomous operation diagnosing of CHP in microgrid. *Applied Thermal Engineering*, 145, 58-70.

Shariati, M., Mafipour, M. S., Mehrabi, P., Zandi, Y., Dehghani, D., Bahadori, A., ... & Poi-Ngian, S. (2019a). Application of Extreme Learning Machine (ELM) and Genetic Programming (GP) to design steel-concrete composite floor systems at elevated temperatures. *Steel and Composite Structures*, 33(3), 319-332.

Shariati, M., Rafiei, S., Zandi, Y., Fooladvand, R., Gharehaghaj, B., Shariat, A., ... & Poi-Ngian, S. (2019b). Experimental investigation on the effect of cementitious materials on fresh and mechanical properties of self-consolidating concrete. *Advances in concrete construction*, 8(3), 225-237.

Shariati, M., Heyrati, A., Zandi, Y., Laka, H., Toghrolfi, A., Kianmehr, P., ... & Poi-Ngian, S. (2019c). Application of waste tire rubber aggregate in porous concrete. *Smart Structures and Systems*, 24(4), 553-566.

Synnefa, A., Santamouris, M., & Livada, I. (2006). A study of the thermal performance of reflective coatings for the urban environment. *Solar Energy*, 80(8), 968-981.

Tevar, J. F., Castaño, S., Marijuán, A. G., Heras, M. R., & Pistono, J. (2015). Modelling and experimental analysis of three radioconvective panels for night cooling. *Energy and Buildings, 107*, 37-48.

Yang, J., Pyrgou, A., Chong, A., Santamouris, M., Kolokotsa, D., & Lee, S. E. (2018). Green and cool roofs' urban heat island mitigation potential in tropical climate. *Solar Energy, 173*, 597-609.

Yew, M. C., Yew, M. K., Saw, L. H., Ng, T. C., Chen, K. P., Rajkumar, D., & Beh, J. H. (2018). Experimental analysis on the active and passive cool roof systems for industrial buildings in Malaysia. *Journal of Building Engineering, 19*, 134-141.

Zhang, S., & Niu, J. (2012). Cooling performance of nocturnal radiative cooling combined with microencapsulated phase change material (MPCM) slurry storage. *Energy and Buildings, 54*, 122-130.

Zhang, L., Fukuda, H., & Liu, Z. (2019). The value of cool roof as a strategy to mitigate urban heat island effect: A contingent valuation approach. *Journal of Cleaner Production, 228*, 770-777.